SULFUR DIFFUSION INTO SOFTWOOD CHIPS

A Thesis
Presented to
The Academic Faculty

by

Gregory Douglas Smith

In Partial Fulfillment
of the Requirements for the Degree
Master of Science in the
School of Chemical and Biological Engineering

Georgia Institute of Technology
December 2005

SULFUR DIFFUSION INTO SOFTWOOD CHIPS

Approved by:

Dr. Sujit Banerjee, Advisor
School of Chemical and Biomolecular Engineering
Georgia Institute of Technology

Dr. Yulin Deng
School of Chemical and Biomolecular Engineering
Georgia Institute of Technology

Dr. Jeff Empie
School of Chemical and Biomolecular Engineering
Georgia Institute of Technology

Date Approved: November 22, 2005

All good things come to those who wait.

To my family and friends – your support makes this possible.

ACKNOWLEDGEMENTS

First, I wish to thank the Institute of Paper Science and Technology along with their member companies for the funding and ability to conduct this research.

I wish to thank my advisor, Sujit Banerjee for providing the insight and guidance for me to accomplish this work. I also wish to thank Aaron Jacobson, with whose help has allowed me a much better understanding of this subject. Jeff Empie deserves recognition for his efforts with the transition of students from IPST to Georgia Tech. Yulin Deng also deserves credit for taking time to help me while he did not have it.

My brother Kyle Smith deserves recognition for his efforts to help me through this. He dealt with the many nights of frustration and struggle from this experience. He made sure that this experience was a fun one as well.

Thanks go to the Western Michigan University department of Paper Engineering for my undergraduate education. I wish to thank the Paper Technology Foundation for their funding during that time. Dr. Raja Avaramuthan should be recognized for instilling a drive and desire for greatness in his students, despite my initial position against it. Dr. Peter Parker should be recognized for guiding me in my undergraduate thesis and encouraging this endeavor to graduate school.

I wish to thank the employees of the Kalamazoo Mill of Graphic Packaging International. Without their help, my first thesis and my quest to grad school would probably not have happened.

Lastly, I would also like to thank Jerry Hoelscher and his fellow employees at Buckman Laboratories for their excellent advice, help with school, and encouragement to attend Georgia Tech.

TABLE OF CONTENTS

		Page
ACKNOWLEDGEMENTS		iv
LIST OF TABLES		viii
LIST OF FIGURES		ix
SUMMARY		xi
CHAPTER		
1	INTRODUCTION	1
2	RELEVANT THEORY AND LITERATURE REVIEW	3
	2.1 Wood Theory	3
	2.2 Wood Pulping Processes	8
	2.3 Kraft Pulping	11
	2.3.1 H-Factor	14
	2.3.2 Batch Digesters	17
	2.4 ABC Test	17
	2.5 Diffusion Theory	19
	2.5.1 Bessel Functions	24
	2.6 Effective Diffusion	26
	2.7 Pretreatment Methods	28
3	EXPERIMENTAL PLAN AND PROCEDURES	32
	3.1 Experimental Design	32
	3.1.1 Chip Moisture	32
	3.1.2 Wiley Mill	32
	3.1.3 Tyler Screening	34
	3.1.4 Soaking	35
	3.1.5 White Liquor Makeup	36
	3.1.6 ABC Liquor Test	37
	3.2 Procedure	39
	3.2.1 Titration Experiments	39
	3.2.2 Equilibrium Analysis	42
	3.2.3 Image Analysis	43
	3.2.4 Effective Diffusion	46
	3.2.5 Tortuosity	47
	3.3 Assumptions	48

4 RESULTS AND DISCUSSION 49

4.1 Summary of Experiments 49
4.2 Fragment Distribution Data 50
4.3 Na_2S Diffusion Time 51
4.3.1 Run 2 51
4.3.2 Run 3 52
4.3.3 Run 4 52
4.3.4 Run 5 and 6 53
4.3.5 Run 7 54
4.3.6 Run 8 54
4.3.7 Run 9 55
4.3.8 Run 10 55
4.3.9 Run 11 56
4.3.10 Run 12 56
4.3.11 Run 13 57
4.4 M_t / M_∞ Calculations 58
4.5 Image Analysis 61
4.5.1 Fragment Size 2.36 – 2.8mm 62
4.5.2 Fragment Size 3.36 – 4.0mm 65
4.6 Effective Diffusivity Calculations 67
4.7 Apparent Tortuosity Calculations 70

5 DISCUSSION OF RESULTS 72

REFERENCES 74

LIST OF TABLES

	Page
Table 2.2.1: Types of Pulping Processes	8
Table 2.5.1.1: Roots of the Zero-Order Bessel Function	26
Table 3.1.3: Tyler Screen Size Fractions	35
Table 4.1: Summary of Experiments	49
Table 4.3.1: Run 2 Data	51
Table 4.3.2: Run 3 Data	52
Table 4.3.3: Run 4 Data	52
Table 4.3.4: Run 5 and 6 Data	53
Table 4.3.5: Run 7 Data	54
Table 4.3.6: Run 8 Data	54
Table 4.3.7: Run 9 Data	55
Table 4.3.8: Run 10 Data	55
Table 4.3.9: Run 11 Data	56
Table 4.3.10: Run 12 Data	57
Table 4.3.11: Run 13 Data	57
Table 4.3.12: Na_2S Stability Over 6 Weeks	58
Table 4.5.1.1: 2.36 – 2.8mm Fragment Sizes	63
Table 4.5.2.1: 3.36 – 4.0mm Fragment Sizes	66
Table 4.6.1: Calculated Effective Diffusion for 2.36 – 2.8mm Fragments	68
Table 4.6.2: Calculated Effective Diffusion for 3.36 – 4.0mm Fragments	69
Table 4.7.1: Calculated Tortuosity Values	70

LIST OF FIGURES

	Page
Figure 2.1.1: Structural View of a Softwood Tree	4
Figure 2.1.2: Average Composition of Softwoods versus Hardwoods	5
Figure 2.2.1: Wood Chipper	10
Figure 2.2.2: 4-Stage Rotary Chip Screen	10
Figure 2.3.1: The Kraft Process	11
Figure 2.3.2: Equilibrium Diagram of White Liquor at Various pH Levels	12
Figure 2.3.1.1: H-Factor Rate versus Temperature (ºC)	16
Figure 2.4.1: Graphical Representation of the ABC Test	18
Figure 2.5.1: Radial versus Axial Diffusion in Cylindrical Coordinates	23
Figure 2.5.1.1: Graphical Representation of Zero and 1st Order Bessel Functions	25
Figure 2.7.1: Modified Polysulfide Cooking Process	31
Figure 4.2.1: Fragment Distribution by Wiley Mill Blade Gap	50
Figure 4.4.1: M_t/M_∞ Data for Run 9	59
Figure 4.4.2: M_t/M_∞ Data for Run 10	59
Figure 4.4.3: M_t/M_∞ Data for Run 11	60
Figure 4.4.4: M_t/M_∞ Data for Run 13 – Short Time Zone	60
Figure 4.4.5: M_t/M_∞ Data for Run 13 – Long Time Zone	61
Figure 4.5.1.1: 8-bit Thresholded Image of 2.36 – 2.8mm Fragments	62
Figure 4.5.1.2: Model of Diffusion Through Actual 2.36 – 2.88mm Fragments	64
Figure 4.5.2.1: 8-bit Thresholded Image of 3.36 – 4.0mm Fragments	65
Figure 4.5.2.2: Model of Diffusion Through Actual 3.36 – 4.0mm Fragments	66
Figure 4.6.1: Effective Diffusivity Analysis for 2.36 – 2.8mm Fragments	68

Figure 4.6.2: Effective Diffusivity Analysis for 3.36 – 4.0mm Fragments 69

Figure 4.7.1: Apparent Tortuosity Values 71

SUMMARY

Environmental concerns and cost reduction have been the focus of pretreatment and extended delignification in Kraft pulping for some time now. Previous work has looked at the diffusion of tritiated water into softwood chips. This thesis looks at the diffusion of Na_2S into southern pine softwood chips. Two size fractions were used. The measured diffusion data were compared to the equilibrium of mixing between the HS^- ion and water alone. Since pine is porous, effective diffusivities were calculated for each size fraction using a 1-dimensional model. Tortuosities were then calculated for the HS^- / pine wood system. These diffusivities are compared to values previously obtained for tritiated water.

CHAPTER 1

INTRODUCTION

The Kraft pulping process has been around since 1884. Since then much focus has been placed on energy conservation and environmental concerns with the pulp and paper industry. One of the biggest spearheads in this effort has been extended delignification. Extended delignification can increase yields for higher profit, lower kappa number so that bleaching chemicals are saved, or pretreat chips so that fewer pulping chemicals are needed.

Much work on pretreatment has been done, but not much on the mechanisms or kinetics involved with such methods. It has been known for a long time that pretreating chips with black liquor containing sulfide would increase yield. Green liquor pretreatment has shown even more promise as the amount of sulfide is even greater. Polysulfide treatments are at the forefront of this movement. In every case, the importance of the sulfide component is shown. To this point, not much work has been done estimating effective diffusivities for sulfide in wood.

Previous work has dealt with the diffusion of tritiated water into chips. This thesis expands upon that work and looks at Na_2S diffusion into softwood southern pine chips. A standard mill white liquor of 106g of active alkali and 30% sulfidity was used on two different size fractions of chip fragments. The first was 2.36 – 2.8mm and the second was 3.36 – 4.0mm. The industry standard ABC titration was used to measure the drop in Na_2S concentration and therefore the diffusion. Several different time scales were used.

A model was developed to compare the chip fragments to cylindrical particles. This model fit very well with less than 5% error when compared to a rectangular particle. A 2-dimensional model was initially proposed but it was later shown that a 1-dimensional model was just as accurate. Image analysis also helped to confirm this.

The diffusion data was then compared to the equilibrium of mixing. This equilibrium results if only the ion component (HS^-) and water were to mix in a large container with no outside effects. Wood is very porous and therefore has a tortuosity associated with diffusion that occurs into it. This porosity was known from previous work. The measured diffusion data was compared to the equilibrium of mixing and an effective diffusivity was calculated. From this effective diffusivity, the tortuosity of the HS^- / pine system was calculated.

The results show that the tortuosity is less than 1.0 for this system. This indicates that something other than Fickian diffusion is taking place in the system. The concept of charge exclusion is introduced as a possible reason.

CHAPTER 2

RELEVANT THEORY AND LITERATURE REVIEW

2.1 Wood Theory

Trees are classified into 2 main categories. The first type is the angiosperm. There are approximately 30,000 types of angiosperm trees in the world. Angiosperms are known as hardwoods as they lose their leaves in winter. The maple tree is an example of a hardwood. In North America, there are approximately 1,200 species of hardwoods [1]. The other type of tree is the softwood also known as a gymnosperm. Softwoods are also called conifers because they retain their needles (leaves) in winter [2]. The southern pine is a softwood species. Figure 2.1.1 shows the anatomy of a typical softwood tree.

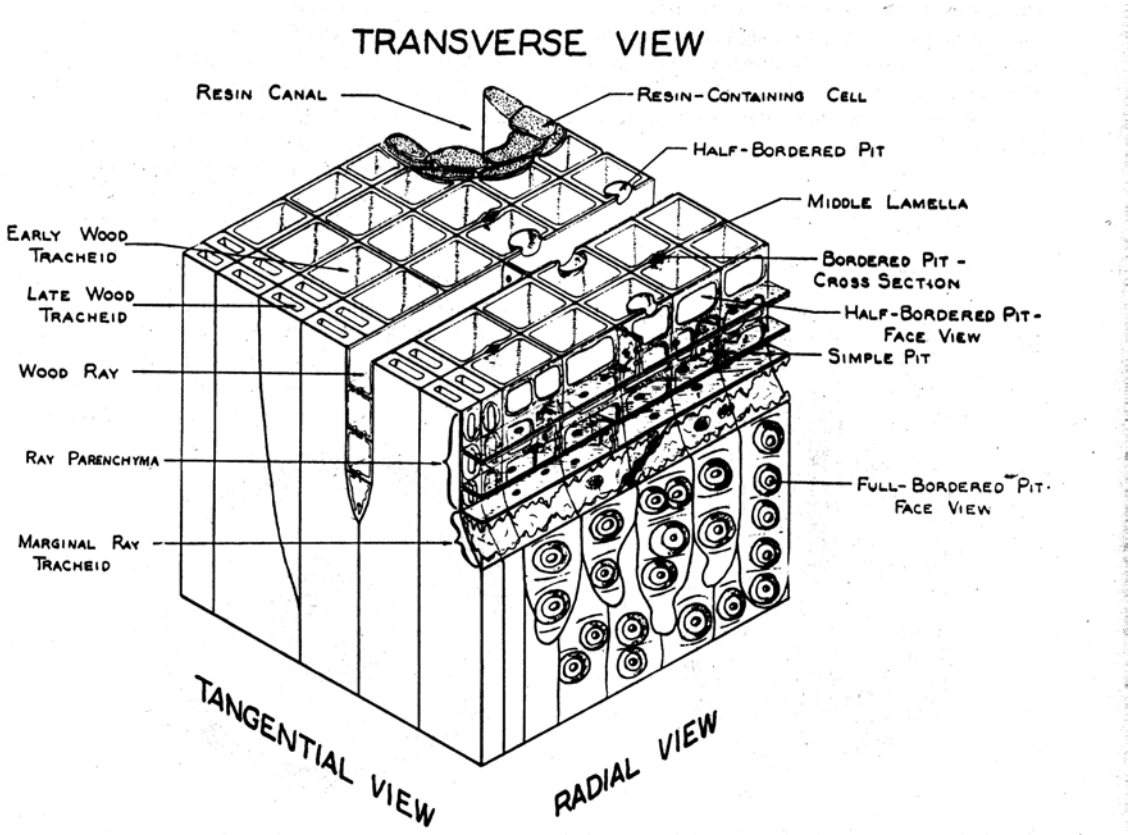

Figure 2.1.1: Structural View of a Softwood Tree [2]

Softwoods are characterized by having cells made up of about 95% fiber tracheids. These tracheids are oriented longitudinally and are typically 3-4mm in length. They are 25-60 μm wide [3]. Hardwood fibers are only 1-2mm in length as a comparison [2]. Tracheids are hollow tubes made of cellulose that are tapered at both ends and are elliptically shaped. They are arranged in radial rows throughout the tree with the tapered ends overlapping longitudinally about ¼ of their length [4].

The fiber walls in softwoods are made up of about 45% cellulose and 30% hemi-cellulose [2]. Cellulose has is a crystalline structure that resists liquid penetration. The degree of polymerization in cellulose is around 10,000. Hemi-cellulose has a degree of polymerization of 100 – 200. It is amorphous, meaning that it allows liquid penetration

[3]. It is therefore easily degraded in pulping. Hemi-cellulose is needed for fiber strength in paper. Strength tests like burst, tensile, and fold are highly dependent on the amount of hemi-cellulose in the paper [2]. Figure 2.1.2 shows the relative amounts of hemi-cellulose and cellulose in softwoods.

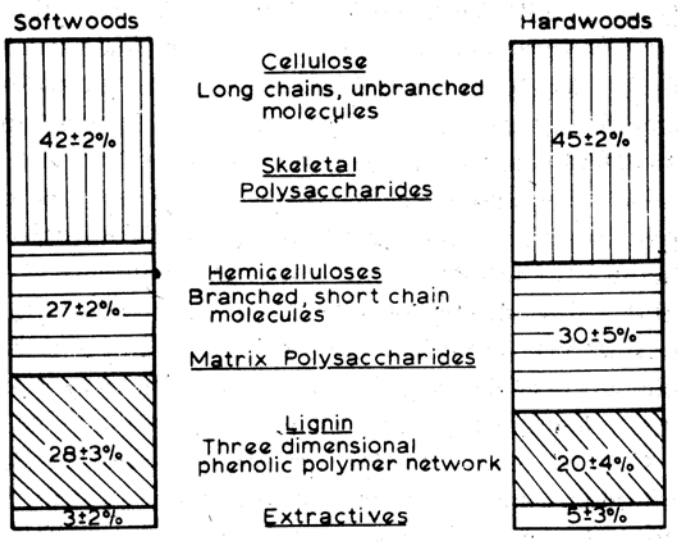

Figure 2.1.2: Average Composition of Softwoods versus Hardwoods [2]

Softwoods have a higher amount of hemi-cellulose than hardwoods (30% versus 27%) [2]. The longer fiber length in softwoods helps paper strength. Paper properties like tear strength depend on fiber length, while smoothness depends on fiber collapsibility. Softwoods build bulk as the fibers do not collapse readily due to their very thick cell walls [3]. As a compromise, many grades of paper are made with a majority of softwood fibers for strength and some hardwood fibers for smoothness.

Softwood cells are made up of 2 layers. The first is the thin outer layer known as the primary wall. The second layer is much thicker and is known as the secondary wall [4]. The secondary wall contains the majority of hemi-cellulose in the fiber. The largest is

known as the S2 layer [1]. The properties of the S2 layer determine the overall strength of the paper. The lumen is the hollow void in the center of the tracheid. It allows for water storage and conduction through the tree [2]. The middle lamella connects the primary walls of different tracheids together. It is mainly composed of lignin [4].

Transport through softwoods takes place via pits (see Figure 2.1.1). These pits cause the wood to have its porous structure [1]. In softwoods, the only intercellular channels for the transport of liquid are the pits [3]. The pit cavity and the pit membrane are the 2 essential components in a pit [4]. The cavity acts as a tunnel for transport to occur through the tracheid while the membrane can block the transport or contain the liquid already inside it. The 2 main types of pits are simple and bordered. In simple pits, the cavity is almost constant in width. In bordered pits, the cavity narrows abruptly toward the cell lumen [4]. If 2 pits are in the walls of adjoining cells they are known as pit pairs. They share a common membrane with 2 primary walls [1]. The pore dimension of the pit in a typical softwood is on the order of 3.5 – 4.0 nm [5]. This is compared with the effective radius of a water molecule at 0.2 nm [6].

Since pits enable the transport in softwood tracheids, they make the otherwise dense wood permeable. Permeability is related to the condition of bordered pit pairs between the longitudinal tracheids in softwoods. Flow in the longitudinal direction in the tree takes place between bordered pits from tracheid to tracheid. These pits are oriented on the radial faces of the tracheids [7]. Typically, there are 50 – 300 bordered pits per tracheid [8]. Flow in the longitudinal direction of the fiber takes place in the fiber lumen [7]. In this way, the transport is observed in only the radial and longitudinal directions. Tangential flow is usually not encountered. For transport to occur tangentially, 300

fibers per cm need to be crossed. In other words, approximately 300 pits in series need to be traversed [7].

Natural wood contains moisture that varies in percentage by tree species, location, and harvest method. This moisture is contained in the cell walls and is either vapor or liquid in the cell cavities [4]. At saturated conditions, there is only liquid in the cell cavities (no vapor is present) [9]. Cell walls become saturated by the hydrogen bonding of water molecules to the hydroxyl molecules in the wood matrix. When the cell walls become fully saturated, water enters the cavities [4]. Water in the cell walls is known as "bound water" and water in the cell cavities is known as "free water." The theoretical point where the cell walls are saturated but the cavities are not is known as the fiber saturation point [10]. It varies between species but is typically 20 – 35% moisture [4].

In wood that is not fully saturated, transport takes place via mass flow through the lumen and then diffusion from the lumen into the cell wall. This process appears to be very rapid [11]. However, this flow comes to a halt when it approaches tracheids at the fiber saturation point or tracheids with lumens that contain liquid-air interfaces [4]. Diffusion can be promoted slightly since the air dissolves into the water somewhat, causing this extra boundary layer to be reduced [12]. Fully saturating the wood ensures that only diffusion takes place since no air voids or extra boundary layers are present [8]. In the past, logs were placed into large ponds for several months before undergoing the pulping process [7]. The ponds would fully saturate the wood and remove any air or extra boundary layers to diffusion.

The penetration of cooking liquors has a profound effect on many pulp properties. Inefficient impregnation results in a higher amount of shives (un-pulped wood

fragments), a higher lignin content at a given yield, and inferior bleachability [13]. Therefore, the penetration of cooking liquor is imperative to a good pulping process. Several techniques can be used to accomplish this. As stated before, fully saturating the fiber is one of the easiest ways. Enzymes can be used as a pretreatment to remove the pit membrane in the tracheids, therefore raising the permeability of the wood and allowing for easier transport [7]. Even the addition of high pH white liquor can raise diffusion by a process called swelling. This is due to the increased accumulation of bound water in the tracheids since the high pH level enhances the adsorption of water. The pits are also swelled so that their diameter increases, allowing for easier transport [4].

2.2 Wood Pulping Processes

Pulping is the process of converting the solid wood mass obtained into useable material by liberating the fibers [1]. There are 3 main types of pulping. Table 2.2.1 shows these types.

Table 2.2.1: Types of Pulping Processes [3]

Mechanical	Hybrid	Chemical
Pulping by mechanical energy (little or no chemicals and heat)	Pulping by mechanical and chemical action	Pulping by chemicals and heat (little or no mechanical action)
High Yield (85 – 95%)	Medium Yield (55 – 85%)	Low Yield (40 – 55%)
Short fibers, wood containing - weak - unstable	Hybrid Pulp Qualities	Long fibers, wood free - strong - stable
Good Print Quality		Poor Print Quality
Difficult to bleach		Easier to bleach

The first is mechanical pulping. This pulp is made by the mechanical action of a machine called a refiner that uses special metal plates to grind the wood mass into pulp. This type is characterized as "wood containing" pulp as the lignin remains with the furnish. Mechanical pulp is cheap and has a very high yield of 85 – 95%. However, the resulting pulp is very weak and discolors over time due to a phenomenon called brightness reversion [14].

The second type of pulping is known as chemical pulping. This type uses chemicals and heat to liberate the fibers. It is also is known as "wood free" pulp as the lignin is removed. This pulp has a low yield (40 – 55%) but is characterized as having a very high strength [2].

The last type of pulping is known as semi-chemical pulping. This type uses a weak chemical pulping (usually green liquor) and is then disintegrated in a refiner with mechanical action. This type of pulp offers a medium yield (55 – 85%) and some unique properties. It is usually only used in liner grades [2].

Logs are harvested from the forest and the debarked. Next they are chipped. Chipping is an extremely important process as most factors in pulping depend on chip thickness. A uniform thickness is needed to ensure chips are not overcooked and yields remain high [2, 3]. Figure 2.2.1 shows a chipper.

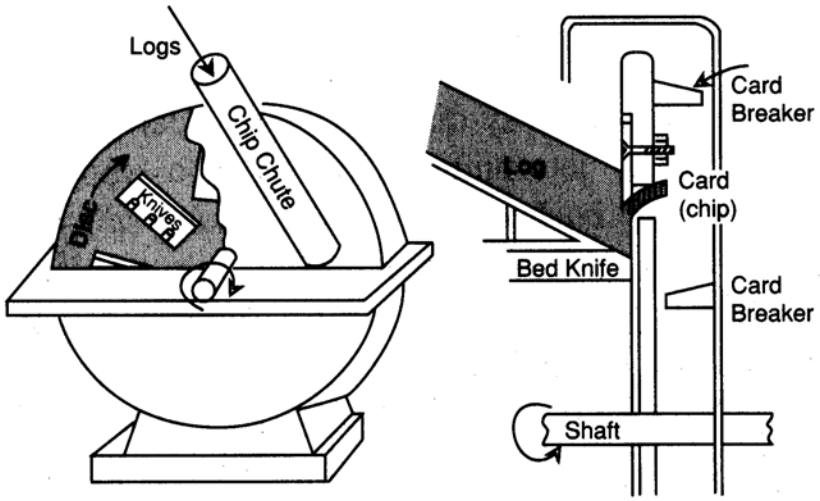

Figure 2.2.1: Wood Chipper [3]

Chips are sorted via thickness by screening. Over-thick chips are narrowed in a chip slicer while under-thick chips are not pulped and are used for energy [2]. Figure 2.2.2 shows a screening system found in a typical mill.

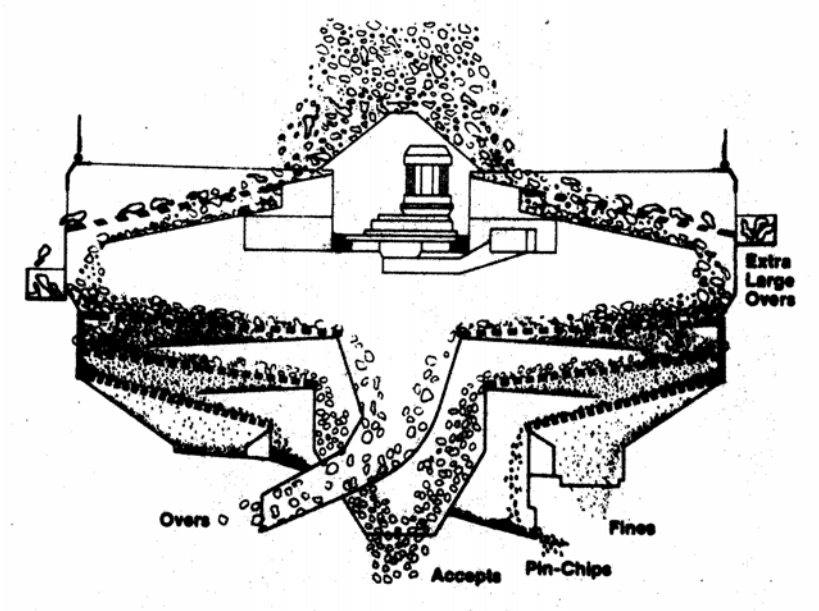

Figure 2.2.2: 4-Stage Rotary Chip Screen [2]

2.3 Kraft Pulping

Kraft pulping is the most popular chemical pulping process in North America [2]. The Kraft process uses sodium sulfide (Na_2S) and sodium hydroxide (NaOH) to dissolve the lignin and free the wood fibers. The temperature used is around 170 ºC.

The chemicals used in this process are expressed in units of Na_2O. This is done so that every chemical used is on an equi-molar basis, but is still measured in units of weight. Weight is much easier to use than a molar basis in a mill. Figure 2.3.1 shows the Kraft process.

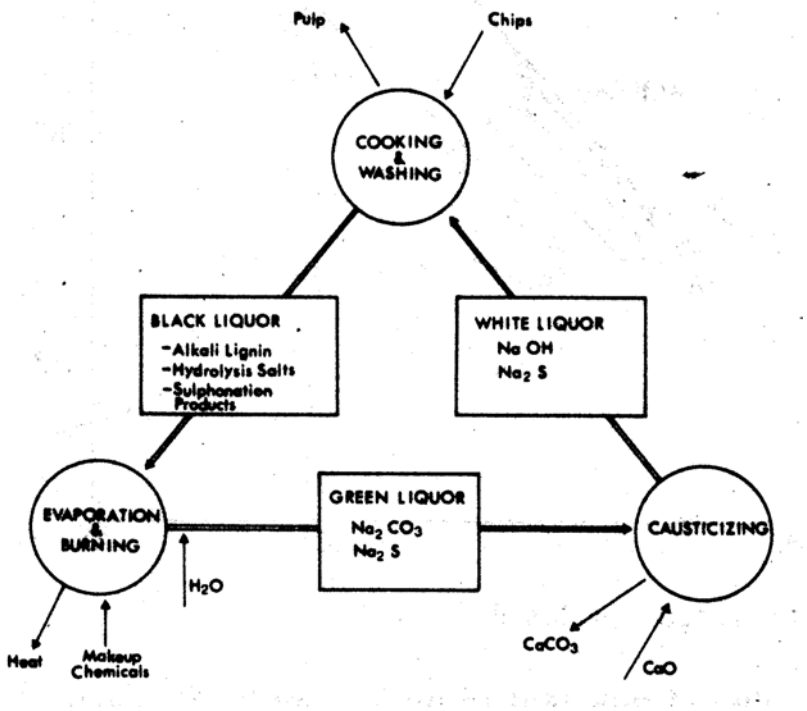

Figure 2.3.1: The Kraft Process [2]

The lignin is split into fragments by the HS^- and OH^- ion. About 80% of the lignin, 50% of the hemi-cellulose, and 10% of the cellulose is dissolved [2]. The following equilibria are observed:

$$S^{-2} + H_20 \leftrightarrow HS^- + OH^- \quad (2.1)$$

$$HS^- + H_20 \leftrightarrow H_2S + OH^- \quad (2.2)$$

The equilibrium constants for these reactions are:

$$K_1 = [HS^-] [OH^-] / [S^{-2}] \quad (2.3)$$

$$K_2 = [H_2S] [OH^-] / [HS^-] \quad (2.4)$$

As seen in the equilibrium equations above, S^{-2}, HS^-, and H_2S all exist in solution [15, 16]. The equilibrium constants for the reaction show that $K_1 >> K_2$. HS^- is the main form of sulfide in the Kraft process, especially at high pH (13 – 14) [1]. Figure 2.3.2 shows this graphically.

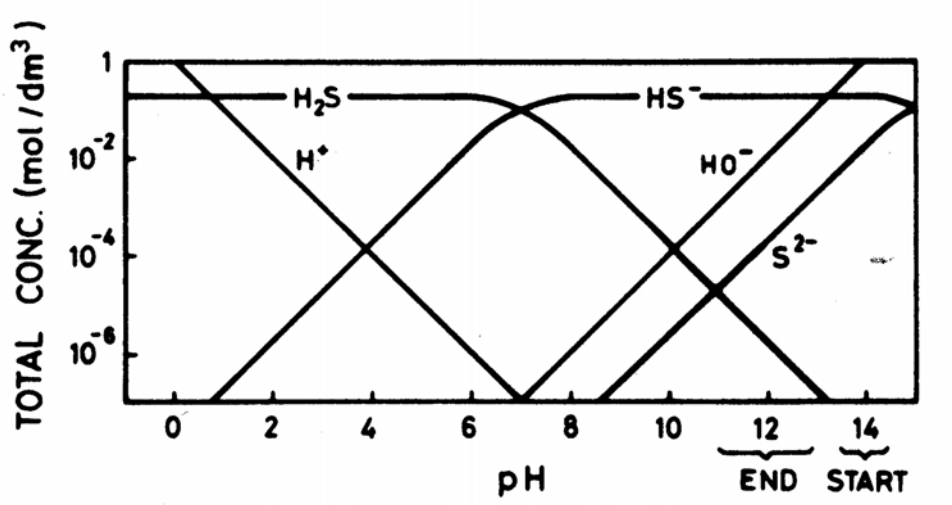

Figure 2.3.2: Equilibrium Diagram of White Liquor at Various pH Levels [1]

Several variables affect the Kraft process. Chip thickness has a direct relationship to screened yield as thin chips over-cook, resulting in severe losses. Thick chips result in shives that lower the yield further [2]. Sulfidity has a pronounced effect on pulping as it protects the wood from hemi-cellulose degradation, raising strength [3]. Temperature is

also very important as the maximum is about 180 ºC before the fibers degrade and lower yields. Liquor to wood ratio (L:W) is also important as enough chemical is needed to ensure adequate penetration [2].

Kraft pulping is done in 3 delignification phases. These are the initial delignification phase, the bulk delignification phase, and the residual phase. The initial phase is characterized by the following equation:

$$\frac{dL}{dt} = A_0 (T)^{½} (\mathrm{e})^{-E/RT} (L) \tag{2.5}$$

where

L = lignin content, % on wood

T = temperature, ºK

t = time, min

A_0 = constant (40)

E = activation energy, cal/mole

R = gas constant

Here it can be seen that the initial phase depends only on diffusion. It does not depend on effective alkali (EA) or sulfidity [17]. The delignification rate depends only on temperature if the pH is above 12 [18]. Since the pH of the initial white liquor concentration is 13 – 14, this condition holds. The values for A_0 and E/R are 40 and 4,807 respectively [17].

In the bulk phase, delignification is first order with respect to lignin [20]. The following equation describes it:

$$\frac{dL}{dt} = A\ (\mathrm{e})^{-E/RT}\ [\mathrm{OH}^-]^{\ a}\ [\mathrm{HS}^-]^{\ b}\ (L) \qquad (2.6)$$

where

$[OH^-]$ = EA concentration at beginning of bulk phase, mole/L

$[HS^-]$ = hydrosulfide concentration at beginning of bulk phase, mole/L

A = frequency factor (7.49×10^{13})

a = reaction order with respect to alkali concentration (0.5)

b = reaction order with respect to hydrosulfide concentration (0.6)

L = lignin content, % on wood

T = temperature, ºK

t = time, min

E = activation energy, cal/mole (29,863)

R = gas constant

Here the delignification is dependent on many factors [17, 19, 20]. The values of E, A, a, and b come from experimental data. The value for E is 29,863, A is 7.49×10^{13}, a is 0.5, and b is 0.6 [17].

2.3.1 H-Factor

Since the preceding equations are rather cumbersome to use in a typical mill, the H-factor is used instead. This is a variable that combines the effect of temperature and time and represents the extent of the delignification in a cook. It is the integral of the relative reaction rate with respect to time. It assumes that active alkali, sulfidity, and other pulping variables are held constant. This is typically the case in a mill. The H-factor rate does not separate the initial and bulk phases, but rather relates the overall cook with an

Arrhenius equation. The H-factor is calculated by the area under the curve of the reaction rate [3]. The rate equation is:

$$k = A\,(\mathrm{e})^{-Ea/RT} \tag{2.7}$$

where

k = rate of reaction

A = pre-exponential factor (43.181)

Ea = Arrhenius activation energy

T = temperature, ºK

R = gas constant

Here A is 43.181 and Ea/R is 16,113. Processes at temperatures below 130 ºC contribute very little to the cook. At 100 ºC, the rate is arbitrarily set at 1. At 25 ºC, it is almost 0 [3]. Figure 2.3.1.1 shows the H-factor rate graphically.

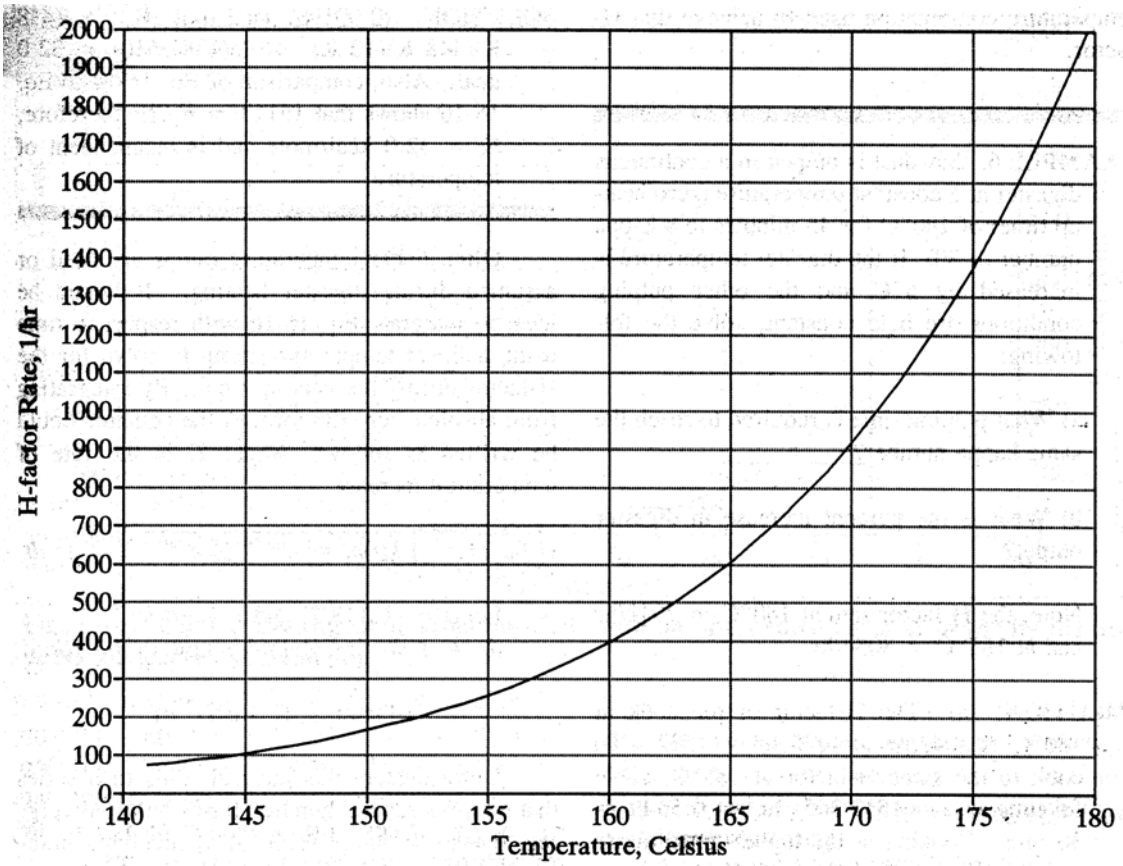

Figure 2.3.1.1: H-Factor Rate versus Temperature (ºC) [3]

2.3.2 Batch Digesters

Batch digesters are relatively old technology. They were used in the first chemical pulping mills in the 1800s. Today, batch digesters still outnumber continuous digesters in North America by about 2:1. This figure is based on the number of mills, not on the number of digesters [22]. Batch digesters have several favorable properties. They are highly reliable as most mills use 8 – 10 of them. They offer better flexibility as one digester can pulp hardwoods while another pulps softwoods. They are also easier to start-up and shut-down [2]. For this reason, laboratory digesters are also of the batch type [23].

Digesters are very tall and narrow. This is mainly so that they take up less floor space and make piping runs shorter. It is also easier since operators are near all of the digesters for operation and maintenance.

Since the batch digester does not allow the wood chips to move like a continuous digester, liquor circulation pumps are used to maintain a constant concentration of liquor around the chips. It also helps maintain consistent temperature. Pressure is also used as a driving force to increase diffusion and impregnate the chips further [3]. Commercial laboratory digesters operate in a similar fashion, but on a much smaller scale. While a mill digester might make up to 19 tons of pulp, the laboratory digester typically makes only a kilogram or two.

2.4 ABC Test

The "ABC titration" is covered in TAPPI 624 cm-00. This test uses white or green liquors at 25 ºC. The resulting titration curve is considered approximate but not exact [3].

For practical purposes, the IPST modified ABC test is used. Figure 2.4.1 shows the principles of the test graphically.

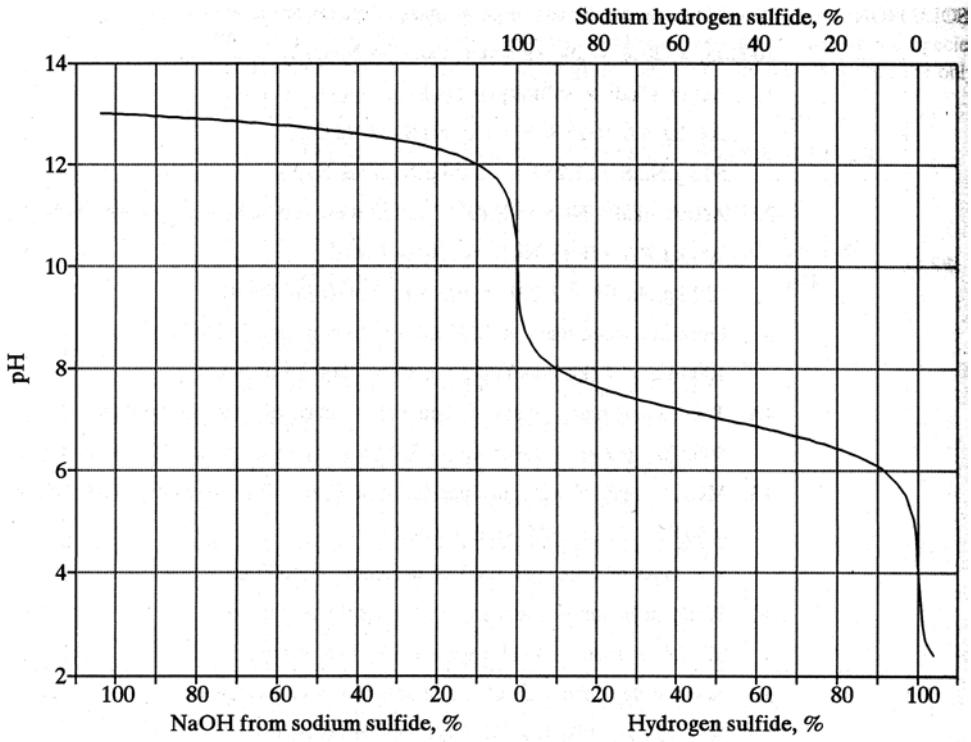

Figure 2.4.1: Graphical Representation of the ABC Test [3]

Initially, the "A" titration is carried out as follows. Excess $BaCl_2$ is added to precipitate any carbonate ion (from green liquor). The reaction is:

$$Ba^{+2} + CO_3^{-2} \rightarrow BaCO_3\downarrow \qquad (2.8)$$

The sample is then titrated with 0.5N HCl acid to an endpoint of 9.3. This represents the effective alkali of the white liquor. During the reaction, Na_2S reacts with water to form NaHS and NaOH. NaHS is a weak base, so the initial phase of the titration only

removes the NaOH and half of the NaHS. Consequently, only half of the Na_2S concentration is measured while all of the NaOH concentration is measured.

In the "B" titration, the remaining Na_2S concentration in solution is measured. The B test therefore measures the active alkali in the white liquor. Excess formaldehyde is added to prevent the formation of H_2S gas (which is highly toxic) and to convert the remaining NaHS to NaOH. Another acid-base titration can then be run similar to the procedure for the A test [3]. The reaction is:

$$HS^- + CH_2O + H_2O \rightarrow CH_2(OH)SH + OH^- \quad (2.9)$$

The pH rises with the liberation of HS^- and the acid titration is run to an endpoint of 9.3. This corresponds to the remaining Na_2S that was in solution [3].

The "C" was not run as white liquor does not contain any compounds that this test measures.

Calculating the concentration of NaOH and Na_2S is done by the following formulas:

$$NaOH = 2A - B \quad (2.10)$$

$$Na_2S = 2\,(B - A) \quad (2.11)$$

2.5 Diffusion Theory

Wood is pulped as chips and the diffusion into these chips occurs in 3-dimensions with the same effective diffusion coefficient. However, only 1-dimension (the thickness) is important to the actual diffusion into the chip. This is due to the large difference in size between the different sides of the rectangle. If the chip is 20mm long, 15mm wide, and only 3mm thick then diffusion will be controlled by the smallest dimension of 3mm.

That is, given a constant diffusion coefficient, the center of the chip (1.5mm) will be saturated in the thickness direction long before the other 2 dimensions become saturated [24].

Although chips are rectangular and use rectangular coordinates for diffusion, fibers can generally be modeled as cylinders. Given their long length of 3-4mm and narrow diameter of 25 – 60 um, they fit this model nicely. Also, since the narrowest dimension is less than a factor of 10 than the longest, this model can be applied [24]. Wood fragments that are used in this thesis are very much like a cylindrical fiber. One size averages 21mm in length, 2.5mm in width, and only 0.98mm in thickness. Since the width is a factor of 10 smaller than the length and the thickness is even smaller, cylindrical modeling can be used [24]. A model is created in Section 4.5 that compares a 3-dimensional rectangular diffusion model to a 1-dimensional cylindrical diffusion model. The 1-dimensional cylindrical model is shown to have less than 5% total error.

The general diffusion equation that models a pulping process must take into account the conservation of chemical species [26]. The general equation is:

$$\frac{\partial C_i}{\partial t} = -\nabla \cdot N_i + R_{vi} \tag{2.12}$$

where

C_i = concentration of species i in molar units

N_i = molar flux of species i relative to fixed coordinates

R_{vi} = net rate of formation of species i, per unit volume

t = time

As in the above statement, cylindrical coordinates are used. If the assumptions of constant density and constant diffusivities are made then the general equation can be modeled as:

$$\frac{\partial C_i}{\partial t} = D_i \nabla^2 C_i + R_{vi} \tag{2.13}$$

where

C_i = concentration of species i in molar units

D_i = diffusivity of species i

R_{vi} = net rate of formation of species i, per unit volume

∇ = the 3-dimensional representation

t = time

If this equation is expanded it becomes:

$$\frac{\partial C_i}{\partial t} + \nu_r \frac{\partial C_i}{\partial r} + \frac{\nu_\theta}{r} \frac{\partial C_i}{\partial \theta} + \nu_z \frac{\partial C_i}{\partial z} = D_i \left[\frac{1}{r} \frac{\partial}{\partial r} \left(r \frac{\partial C_i}{\partial r} \right) + \frac{1}{r^2} \frac{\partial^2 C_i}{\partial \theta^2} + \frac{\partial^2 C_i}{\partial z^2} \right] + R_{vi} \tag{2.14}$$

where

ν_r, ν_θ, ν_z = mass-average velocity with respect to direction of flow

r, θ, z = distance from the center of the particle, measured on each axis

C_i = concentration of species i in molar units

D_i = diffusivity of species i

R_{vi} = net rate of formation of species i, per unit volume

t = time

In a typical mill, this entire equation is likely to be modeled. There is flow in the digester from the liquor circulation pumps, resulting in the retention of the ν_r, ν_θ, and ν_z terms. Also, reaction is taking place so R_{vi} must remain. Since mills often have large distributed control systems and powerful computers, all 3 dimensions can be modeled.

In the laboratory work presented in this thesis, several terms can be eliminated from this general equation. Experiments were performed in small containers that resembled the shape of a batch digester, however no agitation or liquor circulation was provided. This eliminates the ν_r, ν_θ, and ν_z terms from the expression. As expressed before, tangential diffusion is not likely so the concentration gradient in the θ direction can be eliminated [25]. No reaction occurs since the liquor is at room temperature [3]. Effective diffusion dominates since a porous structure is encountered [24]. Also, only a single component is being measured, so only one species is represented (the C_a term). This resulting equation is:

$$\frac{\partial C_a}{\partial t} = D_e\left[\frac{\partial^2 C_a}{\partial z^2} + \frac{1}{r}\frac{\partial}{\partial r}\left(r\frac{\partial C_a}{\partial r} \right)\right] \tag{2.15}$$

where

C_a = concentration of species a in molar units

D_e = effective diffusion coefficient

r, z = distance from the center of the particle, measured on each axis

t = time

However, since the smallest dimension of the particle is a factor of 10 less than the length, radial diffusion can be assumed to be dominate in this process. Section 4.5 shows that the error in such assumption is less than 5%. In other studies, radial and axial

diffusion are compared and it is easy to see that radial diffusion dominates [4]. Particle size was also determined to be dominate in rectangular coordinates as well [25]. Figure 2.5.1 shows axial and radial diffusion for a typical experiment. Here the radial concentration reaches almost 0 after only 6mm (0.4*15) while it takes more than 25mm to approach 0 in the axial position [4].

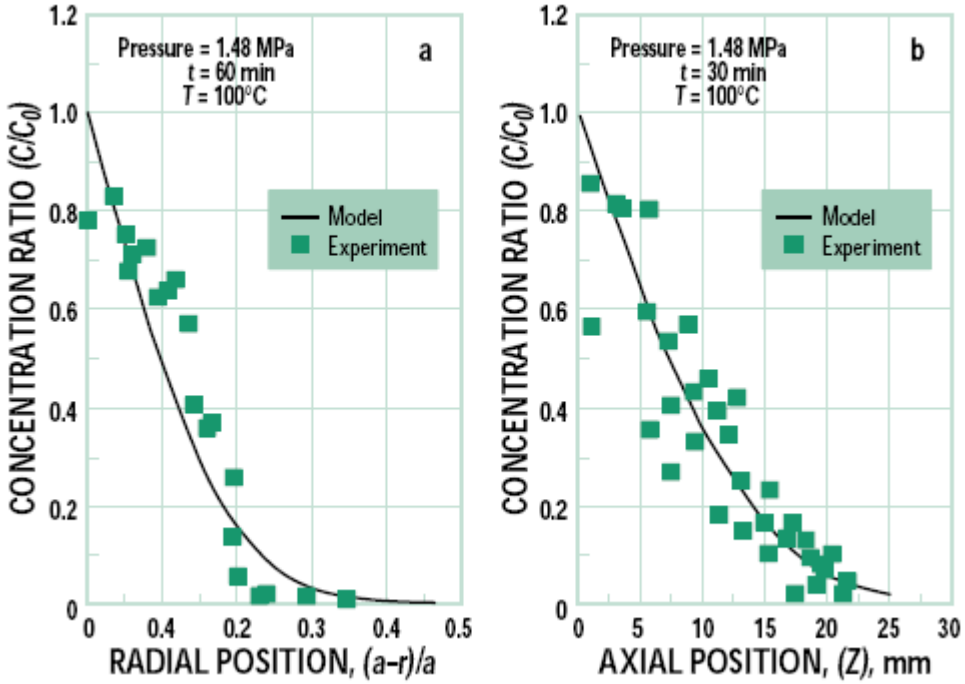

Figure 2.5.1: Radial versus Axial Diffusion in Cylindrical Coordinates [4]
Radius a = 15mm and Length z = 150mm

Since only a 1-dimensional model is used, the new diffusion equation becomes:

$$\frac{\partial C_a}{\partial t} = D_e\left[\ \frac{1}{r}\frac{\partial}{\partial r}\left(\ r\frac{\partial C_a}{\partial r}\ \right)\right] \tag{2.16}$$

where

C_a = concentration of species a in molar units

D_e = effective diffusion coefficient

r = distance from the center axis of the cylinder

t = time

The initial and boundary conditions are:

IC: $C_a = 0$ at $0 \leq r \leq a$ at t = 0

BC: $C_a = C_0$ at $r = a$ at $t \geq 0$

BC: C_a = finite at $r = 0$ at $t \geq 0$

where

C_0 = initial chemical concentration of the white liquor

C_a = chemical concentration of species a at radius r

a = radius of the cylindrical sample, mm

2.5.1 Bessel Functions

Since cylindrical coordinates are used, a second-order differential equation is formed relating the concentration in radius r with time t. This is stated as $C(r,t)$. This equation is an eigenvalue problem and is rather difficult to solve. Bessel functions are a way to solve this second-order differential equation rather easily. In this equation there must be two linearly independent solutions [27]. Since only r is involved with respect to t, the solutions to this equation are Bessel functions of order 0 [26]. Figure 2.5.1.1 shows the zero and first-order Bessel functions and their roots plotted over various x. The roots of the Bessel function of a certain order are the intercepts between the Bessel function curve and the x axis.

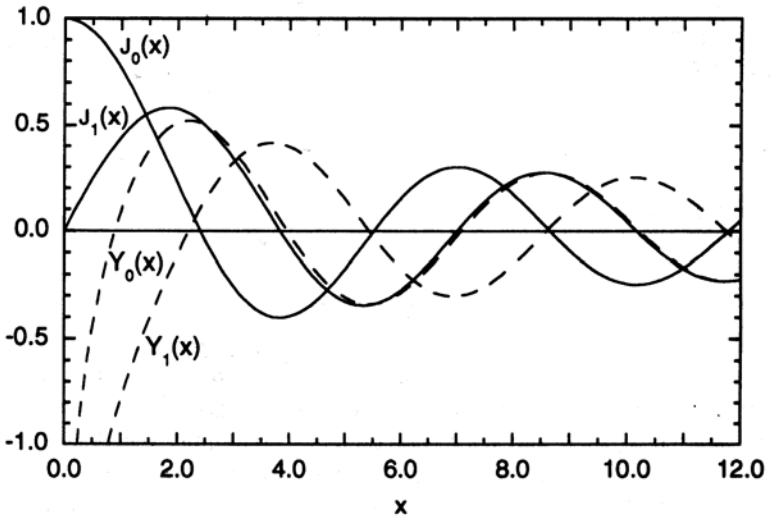

Figure 2.5.1.1: Graphical Representation of Zero and 1st Order Bessel Functions (J_0x) with Derivatives (Y_0x) [26]

If M_t is defined as the mass of solute inside the cylinder at time *t*, and M_∞ is defined as the mass inside the cylinder at infinite time then the required 2 solutions emerge. One is for short periods where $M_t / M_\infty < 0.5$. The other solution is for long times [28]. Since the data collected in this thesis is for $M_t / M_\infty > 0.5$, the solution for long times is used [29].

Another way to think of M_t / M_∞ is as a reaction coordinate. This coordinate is a fraction less than one. It starts from 0 and over time approaches 1.0 at completion. The Bessel function of zero order can be written mathematically as:

$$\frac{M_t}{M_\infty} = 1 - \sum_{n=1}^{\infty} \frac{4}{r^2 \alpha_n^2} \exp\left(-D_e \alpha_n^2 t\right) \tag{2.17}$$

where

M_t = mass of solute inside cylinder at time t

M_∞ = mass of solute inside cylinder at infinite time

r = radius of the fragment

α_n = roots of the Bessel function

D_e = effective diffusion coefficient (calculated)

t = time

The roots for the zero-order Bessel function are:

Table 2.5.1.1: Roots of the Zero-Order Bessel Function [27]

α_n	Zero-Order
1	2.405
2	5.52
3	8.654
4	11.792
5	14.931

In Section 4.5 this equation and the roots were programmed into Excel and the solution was taken to the 5th term [29]. After the 5th term, the resulting solution did not change.

2.6 Effective Diffusion

The typical diffusion coefficient is known as the self-diffusion coefficient (D^o) of mixing. That is, it is measured or calculated as if both components were mixed together in a container with no outside influences. One component would self-diffuse into the other component at the rate measured [24].

Diffusion through porous materials usually results in the self-diffusion coefficient to become inaccurate. The resulting measured coefficient is the known as the effective diffusion coefficient (D_e). Diffusion through a porous material can be of 2 types. Ordinary diffusion occurs when the pore diameter of the material is very large compared

to the diameter of the diffusing substance. The other type is known as Knudsen diffusion. It occurs mostly in gases where the pores of the substance are substantially smaller than the mean free path of the diffusing particles. In other words, the diffusing particles collide more with the pore walls than with other molecules [24]. Since the pore diameter in softwoods is orders of magnitude higher than the diffusing substance, ordinary diffusion takes place.

Porosity (ε) is a unitless number that describes the void fraction in the wood where particles can migrate. The porosity of softwood increases the path the diffusing molecules must travel. This longer path reduces the self-diffusion coefficient and results in an effective diffusion coefficient. This relation to a longer path is known as the tortuosity factor (τ). Tortuosity is a unitless number that describes the impeding effect that porosity has on the self-diffusion coefficient. It can be referred to as a retardation factor [29]. The equation below relates these variables.

$$D_e = \frac{\varepsilon}{\tau} D^{\circ} \tag{2.18}$$

where

ε = porosity - unitless (0.69)

D^o = self-diffusion coefficient of HS^- (1.731×10^{-5} cm^2 s^{-1})

D_e = effective diffusivity (calculated for each experiment)

τ = tortuosity – unitless (calculated)

The porosity in pine was calculated as 0.69 [31]. Since Na_2S was studied in this thesis, the self-diffusion coefficient (D^o) of HS^- is of importance. It was measured to be 1.731×10^{-5} cm^2 s^{-1} at 25 ºC [32].

2.7 Pretreatment Methods

Traditionally, increases in the yield of Kraft pulping were pursued for monetary purposes alone. Today, increased environmental regulations and increases in cost require that mills reduce emissions and increase productivity. The methods proposed were delignifing to a higher kappa number, increasing the cook selectivity to improve strength, and the reduction of carbohydrate losses to increase yield. Several methods are proposed to accomplish such goals [14]. However, most research has been comprised of elementary studies. Not much research has been done on the reaction mechanism or kinetics of pretreatment additives [33].

Black liquor impregnation has been used as a pretreatment process in batch digesters for several years now as a modified cooking process called "Super Batch" [34]. Here chips are added to the digester and weak black liquor (black liquor that has been diluted with brown stock washer filtrate) is added and allowed to impregnate the chips. After this pretreatment, regular white liquor is added and the digester cycle continues. The process is more selective at removing lignin and delignifies to a lower kappa number with 5 – 10% less chemical usage [2].

Since the abundance of sulfide in the low alkaline weak black liquor made so many improvements to the cooking cycle, many have proposed using green liquor instead [34]. The green liquor contains a much higher amount of sulfidity with the same weak alkalinity properties as the black liquor impregnation used in the Super Batch process. In one study, green liquor pretreatment observed a 5% increase in retention of carbohydrates and a 2 – 5% increase in yield. The study also found that green liquor pretreatment resulted in a much lower dependency on sulfidity in the cook. In the study, no observable

change in carbohydrate losses was found down to 1.5% sulfidity [33]. This study shows that the sulfur in the green liquor pretreatment can have profound effects compared to a regular cook. The only drawback is a possibility of increased load on the recovery cycle due to the increased use of green liquor [34].

Polysulfide (Na_2S_x) is another pretreatment chemical that can improve yield. It works to prevent the peeling reaction of carbohydrate end groups much like green liquor pretreatment does. This improves yield and can reduce load on the recovery boiler. Polysulfide can also decrease the kappa number of pulp significantly when used at the same pulping conditions [35]. Polysulfide is usually made by adding elemental sulfur to white liquor in the laboratory. In industrial use, it is made in an oxidizing process known as "MOXY." It is an acronym for the Mead Oxidizing process. Here white liquor is oxidized so that the hydrogen sulfide in the liquor reacts to form polysulfide [36]. The reaction is:

$$(n + 1)\ HS^- + n / 2\ O_2 \rightarrow (n - 1)\ OH^- + S_nS^{-2} + H_20 \qquad (2.19)$$

where

n = number of polysulfide ions from 1 – 5

Polysulfide works very well with the extended delignification process. When 2% polysulfide is added to a regular Kraft cook, a 2.5% yield increase is observed [37]. However, polysulfide decomposes to hydrogen sulfide and thiosulfate at high temperatures. Using polysulfide with a standard white liquor will result in excess sulfur in the system. This sulfur is often emitted as sulfur dioxide in the flue gas of the mill. Due to increasing environmental laws, this is not permissible. Either the sulfidity of the

white liquor used in the cook must be lowered or the polysulfide must be used as only as a pretreatment while regular white liquor is used for the cook [38]. Thiosulfate, although inert, is undesirable as it adds deadload onto the recovery cycle. It was found that using small amounts of manganese dioxide (MnO_2) can reduce thiosulfate generation dramatically [38]. It was also found that too long an oxidation time will form thiosulfate, so process times can be modified to prevent its production [39].

Polysulfide is very attractive as it can be made at a mill using equipment and chemicals that are already present at the site. Several full scale mill trials have been run by using causticizers to produce polysulfide [39]. One study used common air, a single causticizer, and some MnO_2 catalyst to produce the polysulfide. Capital equipment costs were calculated at $2.7 million with annual operating costs of $1.5 million. Using a 2% increase in yield for a 1,000 ton/day mill, benefits of over $11 million could be realized in the first year [40].

Polysulfide is at the forefront of extended delignification. Due to its color it is even termed “orange liquor” now, suggesting that it will serve future Kraft mills much in the way traditional white and green liquors have. The newest proposal using orange liquor technology can eliminate the thiosulfate and low sulfidity problems associated with modifying an existing process. It can even produce polysulfide by oxidation without the use of external oxygen by an electrochemical process. This new process proposes that only high sulfidity polysulfide liquor be added at low temperature at the beginning of the cook. After the polysulfide is allowed to absorb into the chips, straight NaOH is added at high temperature to pulp the chips. After returning through the recovery boiler, excess

hydrogen from the electrolytic cell can be used to produce hydrogen peroxide for bleaching [41]. Figure 2.7.1 shows this process.

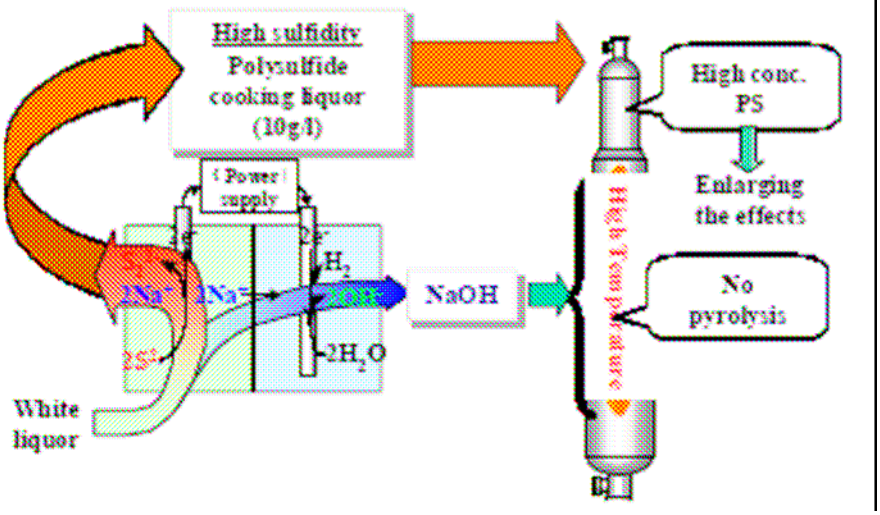

Figure 2.7.1: Modified Polysulfide Cooking Process [41]

Anthraquinone (AQ) should be mentioned as a pretreatment additive. It is an organic compound that works much like a dispersant to improve yield. It is very popular in Asia where wood costs are very high [2]. Yield increases of up to 0.5% can be realized with only a 0.1% addition of AQ [42]. However, AQ is extremely expensive (~$4 per pound) and cannot be made onsite at the mill [2]. Some evidence suggests that a polysulfide/AQ pulping process shows promise. One laboratory study showed a 3% increase in yield with a 1.3% polysulfide / 0.1% AQ cook versus the regular Kraft cook. A 4% yield increase was shown with a 1.6% / 0.1% mix [42].

CHAPTER 3

EXPERIMENTAL PLAN AND PROCEDURES

3.1 Experimental Design

Softwood chips were acquired from the Georgia-Pacific Port Hudson, Louisiana mill through the Institute of Paper Science and Technology. These chips represent a random sample taken after the mill's screening process. They also represent a typical species mix, most likely with a majority of southern pine. The chips ranged in size from 3 – 8mm and were sampled after the mill's slotted screens. They were stored in an air-tight bag in a cold room to prevent decay. The chips were inspected for rot or other deformations to ensure that they were fresh chips and therefore a representative sample.

3.1.1 Chip Moisture

Chip moisture was checked using TAPPI method T 412 om-02 [43]. A cool, dry metal container was obtained and weighed on a scale. 10g of chips were sampled from the collection bag and placed in this container. It was weighed again. The container was placed in a wood drying oven at 105 ºC and left for 24 hours to dry. The container was then quickly removed and weighed. The difference between the wet weight and the dry weight was the chip moisture content. The sampled chips were then discarded.

3.1.2 Wiley Mill

Mill-size chips are not usually good for laboratory work. They are physically very large and have several drawbacks such as increased chemical usage. Therefore chips are fragmented into smaller sizes for laboratory use. The machine that does this is called a Wiley mill. The Wiley mill uses 6 sets of stainless-steel blades that are razor sharp to

fragment wood chips into useable sizes for laboratory use. These blades were recently replaced to ensure accurate cutting and a narrower size distribution. It operates very similarly to a wood chipper found in a mill. A screen is selected based on the desired fragment size and the placed beneath the blades in the collection hopper. Various screens are available with different size holes in them. Hole sizes range from 2 to 10mm. The screen ensures that over-sized fragments are sent through the mill again to be reground.

As the Wiley mill spins, chips are added to the hopper at the top to be fragmented. The mill grinds them into the desired fragment size and then discharges the fragments through the screen and into a collection bag at the bottom. The capacity of the mill is very small, so often times the mill jams. Jams are cleared by removing the chips in the grinding zone and between the blades and placing the material back into the source container. The jammed material is not placed in the collection bag. This way any jammed material is run through the machine again to ensure a narrower size fraction.

The initial expectation was that the diffusion of sulfur was going to take days or weeks to come to equilibrium. Therefore, a very small size wood fragment was needed to keep the diffusion time low. It was decided that the smallest wood fragments possible were needed. Initially the blade gap in the Wiley mill was set to almost zero. The blades had an interference fit to ensure complete fragmentation. A screen size of 2mm was selected as this was the smallest size available. The Wiley mill was run and the resulting fragments were almost particulate. The particles collected were then run through the machine again to ensure they were as small as possible.

When the small size fraction was determined to be detrimental, a larger size fraction was needed. The Wiley mill was then set for two different blade gaps to study the effect

of blade gap on size distribution (Section 4.2). The first gap was 1.5mm and the second gap was 2.5mm. A 10mm screen was used in the mill. This was the largest available. Two different collection bags were used and were labeled accordingly. These bags were air-tight and placed into a cold room when the fragmentation process was complete.

3.1.3 Tyler Screening

Since diffusion is highly dimensionally dependent, an accurate size fraction was needed to ensure accurate diffusion calculations. A vibratory shaker was employed to separate the collected fragments from the Wiley mill into useable size fractions. The vibratory shaker uses 4 Tyler screens at a time with a collection plate on the bottom of the forth screen. The screens employed were hole screens. The unit is turned on and adjusted to the maximum speed. The screens are moved back and forth in one dimension in a very violent fashion. This screening process replicates the hole screens found at a regular mill.

The vibratory shaker was run for ten minutes at a time to ensure adequate fractionation. Screens were placed from largest to smallest. Any material trapped in the screen after a run was discarded to ensure an accurate size fraction. Material in each sized screen was placed into a labeled air-tight bag and placed in a cold room. Material left in the collection screen was then placed in the largest size fraction screen for the next run and the process repeated. A total of 2 complete runs were needed for each size of blade gap. Typically 3 runs were needed to separate all of the material from the Wiley mill. This resulted in a total of 6 runs per size fraction. The entire process was repeated for the 2.5mm blade gap material.

The resulting size distribution was then calculated to determine the effect of blade gap on the resulting distribution (Section 4.2). The material from each set was collected into a tarred container and weighed. This provided the wet weight (at 50% moisture). Using the previously determined moisture content, a dry weight was calculated for the segmented material. Once the information was obtained, the material from each blade gap was combined for a given size fraction. Again, the material was placed in air-tight bags and placed in a cold room to prevent decay. The resulting size fractions and dry weight are listed in Table 3.1.3.

Table 3.1.3: Tyler Screen Size Fractions

Size Fraction	Dry Weight (g)
< 1.0mm	54.4
1.0 – 1.4mm	54.0
1.4 – 1.7mm	53.2
1.7 – 2.0mm	59.9
2.0 – 2.36mm	58.5
2.36 – 2.8mm	111.1
2.8 – 3.36mm	113.6
3.36 – 4.0mm	105.0
4.0mm <	83.9
Total	693.5

3.1.4 Soaking

Since fragments at mill moisture (about 50%) contain large air voids, the fragments were then saturated in water to remove any boundary layers to diffusion. This is necessary to obtain accurate data. The material in each collection bag was placed in a labeled one-liter container full of distilled water. The wood was slightly agitated with a stir rod and a piece of plastic was placed over the opening to prevent decay. The soaking took place at room temperature. The wood was allowed to soak for a total of three days.

After the third day, any fragments floating at the top of the container were decanted and discarded. These floating fragments still contained bound air and therefore were not fully saturated. The resulting solution was then filtered through an 80 mesh screen to separate the wood from the saturation water. The fragments were then washed in running distilled water to remove any particulate matter or extractives present on the wood. The washed fragments were placed into air-tight bags and placed in a cold room.

3.1.5 White Liquor Makeup

A typical mill white liquor was used for every experiment. A goal of 100g of active alkali (AA) and 30% sulfidity was desired. Anhydrous sodium hydroxide (NaOH) was added to a tarred one liter sample container. Sodium sulfide (Na_2S) was then added in a similar fashion. Water was added to make the resulting solution one liter. A mixing rod was added and the solution was allowed to stir until the solids dissolved into solution. Since the resulting mixture is exothermic when formed, careful attention was needed to ensure that the solution was kept away from flammable objects. Since the Na_2S oxidizes in the presence of air, air-tight containers must be used to keep the % sulfidity from degrading.

For the first two experiments (Run 1 and Run 2 – Section 4.3.1) the white liquor that resulted was only 88 g/L of AA and 20% sulfidity. It was likely that the liquor had oxidized in the container. Since this did not meet the specifications of a typical mill white liquor, the solution was discarded. Another solution was made up for the resulting experiments using a better air-tight container. This solution was about 106 g/L AA and 30% sulfidity. Over the course of a month and a half, the sulfidity degraded only slightly indicating the container was much more air-tight than the one used before. Also, a new

procedure of keeping the lid on at all times (except when sampling) proved to be very effective as well.

After 7 weeks it was decided at Run 9 (Section 4.3.6) to add some make-up Na_2S to increase the sulfidity. Only a small amount was needed to move the sulfidity from 28 to 31%. This was the only time any make-up chemical was needed. Further degradation was not noted through the rest of the experiment.

3.1.6 ABC Liquor Test

The ABC liquor test was used to determine the strength of the previously made white liquor. It was also used to measure the diffusion of sulfur into the chips. The ABC test used was an IPST modified test of TAPPI 624 cm-00 [44]. The white liquor container was placed on a magnetic stirrer and allowed to mix for 5 minutes while the titrator was calibrated.

A Mettler DL-21 titrator was used to perform the test. The DL-21 is an electronic titrator with a very high accuracy. It is accurate to +/- 0.3% per titration. The titrator performs an acid-base titration and uses a pH probe to measure the sample. During the titration it adds 0.5N HCl to lower the pH to the desired set-point of 9.3. Once the set-point is reached, the titrator displays the amount of the 0.5N HCl used in mL. This is the result of the test.

The titrator is calibrated by entering the calibration mode and placing the pH probe in pH 4 test solution. The titrator measures pH in the units of mV, so a stable mV reading is needed for an accurate calibration. The DL-21 is programmed to only allow 3mV of drift. This ensures a high level of calibration accuracy. After 5 minutes, a reading is observed and if the reading is at equilibrium, the calibration for that pH is ended. The pH

probe is washed in deionized water and placed in a sample of pH 10 calibration solution. After 5 minutes and a stable mV reading is obtained, the calibration for this pH is ended. The total calibration is then checked manually by placing the pH probe into a pH 7 calibration solution. A measured value of pH 7.0 +/- 0.05 was considered accurate. The DL-21 was calibrated before each experiment.

Once the DL-21 is calibrated, the ABC test can be performed. The ABC test is performed in a hood to prevent noxious sulfur odors and reduce the risk of exposure to H_2S gas. First, a 250mL sample container is obtained and filled with 50mL of distilled water. The 50mL is measured in a graduated cylinder and only an exact amount is allowed. Next a 25mL sample of barium chloride ($BaCl_2$) is added from a measurement cup. A 5mL sample of white liquor is then pipetted from the sample container using a disposable pipette tip. The lid is returned to the sample container immediately. The 5mL amount of white liquor is crucial to the result, so the same pipettor was used throughout all experiments. It was adjusted to 5mL and was found to be both accurate and reproducible. Once the 5mL of white liquor is added, the 250mL sample cup is placed under the mixing device and the pH probe is added. The titration test is started with a target pH of 9.3. Once the pH of 9.3 is obtained, the resulting mL value is the A value of the test.

5mL of formaldehyde is then added to perform the B test. Formaldehyde prevents H_2S gas formation in the test. The same pipettor used for the white liquor is used for the formaldehyde, but a fresh tip is used to prevent contamination. The 250mL sample cup is then placed under the mixing device and another titration is ran. The resulting mL value

is then added to the A value. This gives the B value of the test. Since black liquor was not used in the experiment, the C test was not needed and therefore not run.

3.2 Procedure

3.2.1 Titration Experiments

By using the ABC test and the DL-21 titrator, diffusion into the softwood fragments could be measured. Tests were performed using several 100mL sample containers. These containers were 100mm high. Their shape resembled a standard commercial batch digester very well. The containers were completely air-tight and transparent to allow viewing of the liquor.

First, the main container of fragments was removed from the cold room. A sample container was labeled and then placed dry on a balance and tarred. A sample of fragments was then placed into the sample container. 6.67g of wet fragments (2g OD) were used for each experiment. After the fragments were placed into the container, the lid was replaced so that the fragments would remain at their saturated moisture level. Several more containers were filled (usually 6 to 8) and then placed into a rack for transport. The main container of fragments was then placed back into the cold room. The sample containers were then moved to the DL-21 titrator and allowed to reach room temperature.

Next, the container of white liquor was placed on a magnetic stirrer to ensure a uniform mixture. The ABC test was then performed on the liquor to ensure that no oxidation had taken place and that the liquor was comparable to other experiments in the

series. It was also used as the initial value in each experiment to measure the diffusion taking place. The white liquor was at room temperature for the test.

The time interval of each sample was decided from data taken from before. Initially the time intervals were very large and the sample fragments very small because the diffusion time was thought to be very long. Sample sizes started at 0.6mm and times ranged in hours. As times were found to be much shorter, the time intervals decreased to seconds and the sizes increased to 3.36 – 4.0mm.

Several temporary glass containers were collected and tarred. White liquor was added to these containers based on weight (usually 20g). The white liquor containers were then placed next to the sample containers with fragments. A stopwatch was zeroed and then started as soon as the liquor was added. Each sample container was then sealed and the starting time recorded. The container was left still (no agitation) to prevent any velocity gradients in the system and allow only diffusion to take place.

While the fragment containers were sitting awaiting their testing time a sample cup for an ABC test was prepared. The measured Na_2S concentration from the ABC test would be the result of that time segment. When the exact time was reached, the same pipettor was used with a fresh tip to extract a sample of liquor. Initially in Run 2 and Run 3 (Section 4.3.1 and 4.3.2) the fragments had to be separated from the liquor with filter paper and the resulting solution sampled. Filtration was not needed with the larger size fragments. This sample was taken from the top of the liquor in the sample container to prevent wood particles from entering and ensuring that only liquor was being sampled. The ABC test was run and the test values for that time segment were recorded. Sampling continued until the run was finished.

The goal of running the ABC tests was to measure the diffusion of Na_2S into the size fractions used. Initially, all of the sampled particles reached equilibrium before the measurement was complete. As the measurement time frame shortened from hours to minutes to seconds, a clearer picture of the actual diffusion process developed. As the experiments continued, it was clear the time frame was on the order of seconds as opposed to days. Eventually measurements could be taken before the particles reached equilibrium.

As times became shorter and shorter, singular tests were tried. This involved using a single sample container and sampling 1mL of liquor instead of 5mL for the entire series of tests. The difference in the test values between 1mL and 5mL samples were found to be less than 1%. However, the time to complete the 1mL test was about 2 minutes as compared to almost 15 minutes with the 5mL test. This time savings was considerable when several tests were run at once or short time frames were encountered. The same procedure was followed, but six to seven tests were taken from the same container. This lowered the amount of liquor in the container. Run 5 and Run 6 (Section 4.3.4) showed that this also changed the liquor to wood ratio as the test values for the same time period were different. This method was then abandoned as being inaccurate for final work. It was still used to find the appropriate time scale for a given size fraction.

Sampling then returned to multiple containers. As test times decreased to seconds, individual tests were set up. They were then analyzed and another test was prepared. It was feared that sampled liquor that sat too long would oxidize and make the test inaccurate. This took much longer but was the only way to ensure repeatable results.

As a check, an experiment in Run 12 (Section 4.3.9) was done on an entire chip set horizontally in liquor. This allowed the thickness of the chip to be oriented in the vertical direction similar to the other experiments. Diffusion was allowed in all 3 directions. The check was performed to compare the resulting data for the fragments to an entire chip.

The waste fragments and waste white liquor were then placed in a large 30 gallon container for disposal. Apparatus were then cleaned and readied for future experiments. New experiments were performed with new sample containers.

3.2.2 Equilibrium Analysis

The data collected from the ABC test was organized and placed into an Excel spreadsheet broken down by each Run (Section 4.4). Run conditions were noted and the resulting data were then placed into a spreadsheet.

The spreadsheet of Na_2S concentration versus time was then graphed. The equilibrium line on the graph was calculated by the following formula:

$$C_1 * V_1 = C_2 * V_2 \tag{3.1}$$

where

C_1 = initial concentration of white liquor in the experiment (measured)

V_1 = volume of white liquor in the experiment by weight (20 g)

C_2 = calculated concentration of equilibrium by mixing only

V_2 = volume of white liquor and volume of H_2O in wood by weight (24.7 g)

This equation was then used for each experiment to find the equilibrium of mixing. The initial concentration of the white liquor C_1 was measured in the initial ABC test of

each experiment. The equilibrium line was then found by solving for C_2. V_1 and V_2 remained constant for each experiment as the L:W ratio was the same.

The M_t / M_∞ data for a particular data point was calculated by the following formula:

$$M_t / M_\infty = 1 - \frac{C_x - C_{eq}}{C_0 - C_{eq}} \tag{3.2}$$

where

M_t = mass of solute inside cylinder at time t

M_∞ = mass of solute inside cylinder at infinite time

C_x = measured Na_2S concentration at time x

C_{eq} = equilibrium of mixing

C_0 = concentration of Na_2S at time 0

This formula was used to calculate the M_t / M_∞ at each data point. Each time segment had a resulting M_t / M_∞ value. By subtracting the fraction from 1, the resulting data range from 0 to 1.0 much like a reaction coordinate. These points were then used in Section 4.6 to calculate the effective diffusivities.

3.2.3 Image Analysis

In order to confirm that the sampled particles were indeed cylindrical, image analysis was performed on a sample of fragments used in each experiment (Section 4.5). A sample of 96 2.36 – 2.8mm fragments and a sample of 97 3.38 – 4.0mm fragments were acquired. These fragments were placed onto a white piece of paper and aligned so that they were all vertical. A metric ruler was placed at the top of the paper as a reference. An ultra-high resolution photograph (2048 X 1586 pixels) was taken of the resulting

sample. The size of this photograph was over 9MB. A typical resolution photograph ranges in size from 0.2 to 0.5 MB.

Since the photograph could only see two dimensions, the third dimension (width) was measured using a dial caliper on all of the sample fragments. This dial caliper was zeroed and accurate to +/- 0.001 inches. Data was recorded and then converted into millimeters.

A public domain image analysis software was used to analyze the 2 dimensional photographs. This software was developed by the National Institute of Health and is called ImageJ [45]. The 1.34s version of ImageJ was used to analyze the photographs. The photograph was loaded into ImageJ and then converted into 8-bit grayscale (from 32-bit color). A reference line was drawn onto the ruler in the image so that the ImageJ program had a known reference length. The image was then thresholded via an algorithm in ImageJ to separate the particle images from background noise. The particle area was then selected and image analysis was done. The measured values were area, feret, major and minor ellipse measurements, and perimeter. This was done for each individual particle.

ImageJ uses an "Edge" command that can help the particles stand out better and make the thresholding process more accurate. Measurements were taken with and without the Edge feature, and the difference was negligible. The Edged data were then used in the analysis.

A spreadsheet was created in Excel combining the 2-dimensional data from ImageJ and the measured width to encompass a 3-dimensional picture of the particles. Average

and median were calculated for each value. The values were very close, so the average result was used in the calculation.

A model was created comparing the actual rectangular particle to the theoretical cylindrical particle that was being modeled. The penetration depth (P_x) was studied every .01mm in both particles. It was squared to represent penetration from either direction. It was increased until the rectangular particle reached 100% saturation.

Since the penetration depth was now known for the rectangular particle a corresponding depth could be found for the cylindrical particle. The model was run by comparing the diffusion in an actual average particle size (length, width, and height) with a cylinder of radius *r* with the same length. A sample *r* (guess) was entered into the spreadsheet. The sum of squares difference between the rectangular and cylindrical model was then calculated. Excel Solver was used to calculate the *r* of the cylinder that minimized this sum of squares difference. By minimizing the difference, a theoretical cylinder could be found that replicated the diffusion characteristics of the actual rectangular particle. Section 4.5 shows the results. The formula for the rectangular particle of either size was:

$$3D_x = \frac{V - \left[\left(l - P_x^{\,2}\right) * \left(w - P_x^{\,2}\right) * \left(h - P_x^{\,2}\right)\right]}{V} \tag{3.3}$$

where

$3D_x$ = total diffusion in the rectangular particle at penetration depth *x* (%)

V = volume of rectangular particle (mm^3)

P_x = penetration of diffusant (mm)

l = average length of rectangular particle (mm)

w = average width of rectangular particle (mm)

h = average height of rectangular particle (mm)

The corresponding formula for the cylinder was:

$$1D_x = \frac{V - \left[\pi * (r - P_x)^2 * (l)\right]}{V} \tag{3.4}$$

where

$1D_x$ = total diffusion in the cylindrical particle at penetration depth x (%)

V = volume of cylindrical particle (mm^3)

P_x = penetration of diffusant (mm)

r = sum of squares difference calculated radius r (mm)

l = average length of rectangular particle (mm)

3.2.4 Effective Diffusion

The effective diffusion coefficient (D_e) was calculated using the formula:

$$\frac{M_t}{M_\infty} = 1 - \sum_{n=1}^{\infty} \frac{4}{r^2 \alpha_n^2} \exp\left(-D_e \alpha_n^2 t\right) \tag{3.5}$$

where

M_t = mass of solute inside cylinder at time t

M_∞ = mass of solute inside cylinder at infinite time

r = radius of the fragment

α_n = roots of the Bessel function

D_e = effective diffusion coefficient (calculated)

t = time

This summation was programmed into an Excel spreadsheet and was taken using time from 1 to 440 seconds (Section 4.6). Every value is known except for D_e. The summation was taken as the theoretical solution and is plotted as the "Equilibrium of Mixing Only" on all of the graphs.

The VLOOKUP function was used in Excel to match the M_t / M_∞ values from experimental data to the theoretical value in the formula based on time (in seconds). Only an exact match was allowed. The sum of squares difference was calculated between the theoretical and the actual M_t / M_∞ data. Excel Solver was then used to change the D_e value to make the total sum of squares difference as close to zero as possible. The actual M_t / M_∞ data points were then plotted versus the theoretical equilibrium of mixing so comparisons could be made. The resulting D_e value changed for each experiment as each data set was different.

3.2.5 Tortuosity

The tortuosity was then calculated using the formula:

$$D_e = \frac{\varepsilon}{\tau} D^\circ \tag{3.6}$$

where

ε = porosity - unitless (0.69)

D^o = self-diffusion coefficient of HS^- (1.731×10^{-5} cm^2 s^{-1})

D_e = effective diffusivity (calculated for each experiment)

τ = tortuosity – unitless (Calculated)

The porosity for pine is 0.69 [31]. The self-diffusion coefficient (D^o) and D_e values were both known. D^o was found from published data [32] and the D_e was calculated from the experimental data. The resulting tortuosities were compared by size fraction.

3.3 Assumptions

A few assumptions were made in this thesis. These include:

- No reaction takes place since the temperature is so low
- Diffusion into chips takes place in all 3 directions at equal rates, but the thickness (or radius of the modeled cylinder) is the critical dimension
- The decrease in liquor composition can describe the diffusion into the fragment
- No temperature gradients exist within the fragment
- Wood is treated as lignin and carbohydrates – no distinction is made between different types of each component
- The sulfide in the liquor completely hydrolyzes to HS^-
- Excess extractives in wood have been removed by the washing process

CHAPTER 4

RESULTS AND DISCUSSION

4.1 Summary of Experiments

Table 4.1 shows a summary of each experimental Run and the conditions attached to it. Data from Run 9, 10, 11, and 13 are used in the calculation of tortuosity. Run 9 shows the resulting diffusion values for the 2.36 – 2.88mm fragments. Run 11 shows the resulting diffusion values for the 3.36 – 4.0mm fragments. Run 12 is an experiment with a 3 – 6mm whole chip. Run 13 is an extended time study of the diffusion of the 3.36 – 4.0mm fragments.

Table 4.1: Summary of Experiments

Run	Size Fraction (mm)	OD g Wood	g Liquor	L:W	Liquor AA (g/L)	Liquor Sulfidity	Test Type	Sample Size
2	0.5 - 0.8	2	10	5:1	88	20%	Individual	5 mL
2	0.8- 1.0	2	10	5:1	88	20%	Individual	5 mL
3	0.8 - 1.0	2	10	5:1	106	30%	Individual	5 mL
4	2.36 - 2.8	2	20	10:1	107	30%	Individual	1 mL
5	2.36 - 2.8	2	20	10:1	107	30%	Single	1 mL
6	2.36 - 2.8	2	20	10:1	107	30%	Single	1 mL
7	2.36 - 2.8	2	20	10:1	111	28%	Single	1 mL
8	2.36 - 2.8	2	20	10:1	93	29%	Single	1 mL
9	2.36 - 2.8	2	20	10:1	105	32%	Individual	5 mL
10	3.36 - 4.0	2	20	10:1	90	33%	Single	1 mL
11	3.36 - 4.0	2	20	10:1	105	32%	Individual	5 mL
12	3 - 6 chip	2	20	10:1	95	30%	Individual	1 mL
13	3.36 - 4.0	2	20	10:1	104	32%	Individual	5 mL

4.2 Fragment Distribution Data

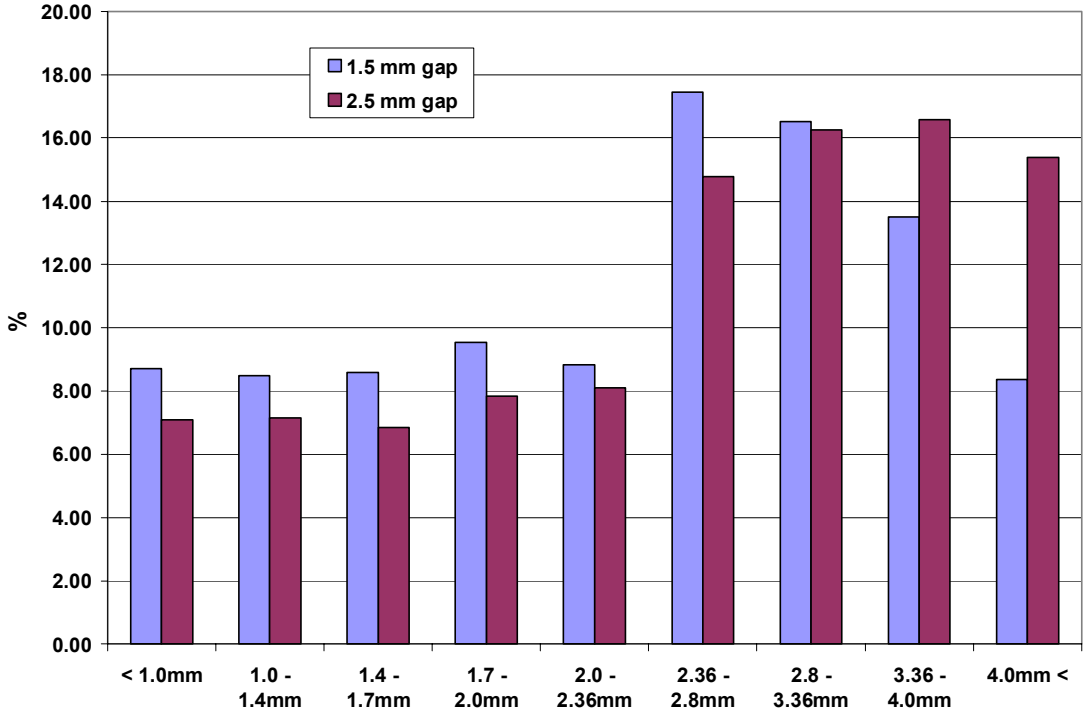

Figure 4.2.1: Fragment Distribution by Wiley Mill Blade Gap

Figure 4.2.1 shows the results of changing the blade gap of the Wiley mill. As expected, a 1.5mm blade gap showed a peak distribution in the 2.36 – 2.8mm size range. The 2.5mm blade gap showed a peak distribution in the 3.35 – 4.0mm size range. The results of this distribution contributed largely on the choice of fragment sizes in the experiment. A large enough amount of wood would be needed to run all of the experiments, so the peak distribution of each blade gap was chosen.

It is interesting to note that while the 2.5mm blade gap has the majority of the fragments that size or larger, there is still a significant amount of fragments that are below this size. This result shows why accurate screening is so important. Since

diffusion is largely size related, an inaccurate sample of fragments would make the resulting data inaccurate.

4.3 Na_2S Diffusion Time

Several experiments were run to measure the diffusion of Na_2S into the softwood fragments of different size fractions. Table 4.3.1 – 4.3.3 (Run 2 – Run 4) show data that the equilibrium was reached before any measurement could take place. The resulting tables (Table 4.3.4 – Table 4.3.11) show the measured diffusion data for different particle sizes and times.

The zero value in each table is the initial ABC test on the white liquor to determine the starting concentration for that experiment. It was also taken to determine if any oxidation had taken place between the last test. Fragments were not added for the zero test, but were used in the resulting time segments.

4.3.1 Run 2

Run 2 used particle sizes of 0.5 – 0.8mm and 0.8 – 1.0mm in a time scale of several hours.

Table 4.3.1: Run 2 Data

0.8 – 1.0mm

Sample	0	2 hr	4 hr	5.5 hr	24 hr	48 hr
Na_2S	**18.06**	**9.27**	**8.88**	**9.67**	**8.23**	**7.61**
Sulfidity %	20.43	21.09	20.01	20.34	18.28	16.47

0.5 – 0.8 mm

Sample	0	2 hr	4 hr	5.5 hr	24 hr	48 hr
Na_2S	**17.20**	**7.32**	**9.31**	**8.71**	**8.01**	**7.30**
Sulfidity %	20.40	20.84	20.17	20.97	18.40	16.07

4.3.2 Run 3

Run 3 used the same 0.8 – 1.0mm sized particles as in Run 2. However, since Run 2's white liquor did not approximate a mill liquor adequately, a new batch of white liquor was made up at 106g/L AA and 30% sulfidity.

Table 4.3.2: Run 3 Data

0.8 – 1.0mm

Sample	0 min	5 min	10 min	20 min	30 min	40 min	50 min	60 min	70 min
Na_2S	**32.65**	**19.03**	**18.51**	**18.01**	**18.53**	**18.56**	**17.80**	**17.05**	**17.42**
Sulfidity %	30.74	33.96	33.70	35.34	34.16	34.18	33.75	33.68	33.92

4.3.3 Run 4

After another round of Wiley mill grinding and separating through the Tyler screens, the 2.36 – 2.8mm fragments were ready for testing. Sampling became a concern with the short sample times encountered in this test. An initial fear was that sampling occurred much more frequently than a test could be run. For example, a 5mL sample size would take 10 – 15 minutes to analyze. Since samples were being taken every few minutes, it was feared that the sampled liquor would oxidize in that short amount of time making the resulting test values inaccurate. In order to speed up the ABC testing process, 1mL samples were taken to ensure that no oxidation took place in the acquired samples. It was decided that a short time frame (0 – 5 minutes) and a longer time frame (15 – 75 minutes) should be used to measure the diffusion.

Table 4.3.3: Run 4 Data

2.36 – 2.8mm

Sample	0 min	1 min	2 min	4 min	5 min	10 min	15 min	20 min	30 min	45 min	60 min	75 min
Na_2S	**32.55**	**28.37**	**27.98**	**28.22**	**26.55**	**25.76**	**25.61**	**25.69**	**24.63**	**26.62**	**25.04**	**25.18**
Sulf %	30.24	31.27	31.80	32.33	31.44	31.71	31.75	31.44	32.48	30.81	31.04	30.31

4.3.4 Run 5 and 6

For Run 5 and 6 the same fragment size and white liquor was used. The 1mL ABC test size proved to be quite effective in preventing oxidation of the sample and speeding up the sampling process. The time scale measured was going to be a total of 2 minutes. Since the time scale between samples was too small, it was feared that oxidation would occur. To combat this, a singular test was run. This meant that all samples for each data point were taken from a common sample container instead of from many individual containers.

Table 4.3.4: Run 5 and 6 Data

2.36 – 2.8mm

Sample	0	10 sec	20 sec	30 sec	40 sec	50 sec	60 sec	70 sec
Na_2S	**32.29**	**26.33**	**23.59**	**24.47**	**25.33**	**24.78**	**24.92**	**25.53**
Sulfidity %	30.05	29.07	28.53	29.02	30.15	31.08	29.61	31.39

2.36 – 2.8mm

Sample	0	70 sec	80 sec	90 sec	100 sec	110 sec	120 sec
Na_2S	**32.29**	**29.34**	**27.95**	**28.01**	**28.08**	**30.59**	**28.44**
Sulfidity %	30.05	30.61	30.09	30.21	29.95	30.87	31.29

One problem was noted with this singular testing method. The time segment of 70 seconds has two different measured concentrations between runs. In Run 5, the result is 25.5g/L and in Run 6 it is 29.3g/L. As the test progressed, less liquor was in the sample

container from samples being withdrawn from it. This lowered the L:W ratio as the experiment progressed. The lower L:W ratio at the end of Run 5 caused a larger drop in concentration than what would normally be observed in a constant L:W ratio test. Evidence of this is found in Run 6, where the 70 second sample point is the first test and the L:W ratio is still very high.

4.3.5 Run 7

Run 7 uses the same 2.36 – 2.8mm particle sizes in a shorter time scale. The shorter scale was used since the diffusion was progressing so rapidly in Run 6 (Table 4.3.4).

Table 4.3.5: Run 7 Data

2.36 – 2.8mm

Sample	0	5 sec	10 sec	15 sec	20 sec
Na_2S	**31.36**	**31.50**	**28.81**	**31.48**	**34.66**
Sulfidity %	28.25	28.78	29.31	29.50	30.19

4.3.6 Run 8

Run 8 uses an even shorter time scale. However, since the measurement technique for such short time scales was not perfected yet, the closest time frame was 3 seconds between samples. This test used a single sample, so it was decided that future tests with such a short time scale needed to be individual tests so that samples could be taken every second.

Table 4.3.6: Run 8 Data

2.36 – 2.8mm

Sample	0	3 sec	6 sec	9 sec
Na_2S	**27.31**	**22.83**	**28.94**	**31.70**
Sulfidity %	29.36	29.69	29.18	29.88

4.3.7 Run 9

Run 9 used individual tests and 5mL samples to measure the diffusion of the 2.36 – 2.8mm fragments. Since individual tests were used, sample intervals of one second could be measured. The Na_2S concentration dropped a total of 3.4g/L or 10.1%.

Table 4.3.7: Run 9 Data

2.36 – 2.8mm

Sample	0 sec	1 sec	2 sec	3 sec	4 sec	6 sec	9 sec	12 sec	1 hr	2 hr
Na_2S	**34.33**	**33.11**	**32.69**	**30.86**	**32.64**	**31.03**	**31.03**	**32.46**	**25.31**	**25.48**
Sulfidity %	32.70	32.87	33.17	33.34	32.67	33.43	33.51	33.42	32.62	32.39
Change Na_2S %	100.00	96.42	95.20	89.88	95.05	90.38	90.39	94.55	73.71	74.21

4.3.8 Run 10

Run 10 shows the measured diffusion data for the 3.35 – 4.0mm fragments. A singular test with 1mL samples was run to determine if the larger fragments would exhibit different behavior from the smaller 2.36 – 2.8mm fragments. The time scale was extended since it was not certain what effect size would have on the measured diffusion.

Table 4.3.8: Run 10 Data

3.36 – 4.0mm

Sample	0	5 sec	10 sec	15 sec	20 sec	25 sec	30 sec
Na_2S	**29.57**	**20.84**	**26.97**	**22.79**	**25.67**	**21.47**	**24.87**
Sulfidity %	33.03	29.86	30.27	31.17	30.27	30.61	31.70

4.3.9 Run 11

Run 11 used individual tests and 5mL samples for an accurate measurement of the diffusion into the fragments. Since an individual test was run, the time scale could be reduced to a single second. The Na_2S concentration dropped a total of 4.9g/L or 14.5%.

Table 4.3.9: Run 11 Data

3.36 – 4.0mm

Sample	0 sec	1 sec	2 sec	3 sec	4 sec	5 sec	6 sec	7 sec	10 sec
Na_2S	**33.52**	**31.65**	**31.87**	**31.42**	**30.21**	**28.66**	**31.51**	**31.56**	**30.89**
Sulfidity %	31.95	31.16	31.84	31.76	31.54	32.02	31.64	31.33	31.85
Change Na_2S %	100.00	94.43	95.09	93.74	90.14	85.51	94.02	94.17	92.15

4.3.10 Run 12

Run 12 was done as a check to ensure that the data from the two sample sizes agreed with an actual chip. Actual chips were not part of the original research plan, but if the data from a whole chip matched that of the fragments, it would help verify that the fragment data is correct.

An entire 3 – 6mm width chip (with a length of 20mm and width of 15mm) was sampled from the original supply of southern pine. This chip was placed unaltered so that it rested horizontally in the sample container. The width of the chip was placed in the vertical direction so that the test was run similar to the tests with fragments. This also allowed the entire chip to be submerged in the same amount of liquor used in the other experiments. Diffusion was allowed in all three dimensions.

Table 4.3.10: Run 12 Data

3 – 6mm Chip

Sample	0	5 sec	10 sec	15 sec	20 sec
Na_2S	**28.49**	**26.98**	**29.16**	**26.82**	**30.85**
Sulfidity %	30.05	30.52	31.22	30.82	31.01
Change Na_2S %	100.00	94.72	102.35	94.15	108.31

Since the chip is a similar size to the larger fragments, the diffusion data measured is very similar.

The measured drop in Na_2S concentration is 1.5g/L or 5%, which is not as large as what was measured in both the 2.36 – 2.8mm (Run 9 – Table 4.3.7) and the 3.35 – 4.0mm (Run 11 – Table 4.3.9) fragment sizes.

4.3.11 Run 13

An extended time study was done based on data measured previously. The study used the same 3.36 – 4.0mm fragment size used in the experiments prior. The same white liquor concentrations were used. A short time study was done to help verify the data already collected. A longer time study was done to see where the Na_2S concentration leveled completely. This was expected to take several days to happen. Table 4.3.11 shows the data.

Table 4.3.11: Run 13 Data

3.36 – 4.0mm

Sample	0 sec	5 sec	30 sec	5 min	15 min	30 min	1 hr	1 day	3 day	5 day	7 day	14 day	21 day
Na_2S	**32.00**	**29.48**	**30.03**	**28.51**	**27.36**	**26.97**	**26.21**	**24.60**	**23.94**	**23.54**	**22.84**	**22.69**	**22.71**
Sulfidity %	30.77	31.16	31.27	33.18	33.86	33.09	32.42	31.45	30.85	30.72	30.41	30.41	30.41
Change Na_2S %	100	92.11	93.83	89.08	85.48	84.27	81.89	76.87	74.79	73.55	71.37	70.90	70.95

Unlike in the previous experiments, the concentration finally leveled after 14 days. A check was done after 21 days to confirm that the concentration had stabilized. The total drop in Na_2S concentration was 9.3g/L or 29.1%. Since the drop in white liquor concentration was so low using the new air-tight containers in previous experimentation (based on the previous observation of only adding Na_2S after 6 weeks) oxidation was not feared to take place in the short time frame of 3 weeks. Any drop in Na_2S concentration was therefore due to diffusion and not oxidation.

Further proof of this can be found in Table 4.3.12. This table shows Run 3 through Run 8. This experimentation took about 6 weeks. It can be seen that the AA and Sulfidity is the same over the 5 week period, with only a little make-up Na_2S needed at week 6.

Table 4.3.12: Na_2S Stability Over 6 Weeks

Week	Size Fraction (mm)	Liquor AA (g/L)	Liquor Sulfidity
1	0.8 - 1.0	106	30%
2	2.36 - 2.8	107	30%
3	2.36 - 2.8	107	30%
4	2.36 - 2.8	107	30%
5	2.36 - 2.8	111	28%
6	2.36 - 2.8	93	29%

4.4 M_t / M_∞ Calculations

The M_t / M_∞ graphs show a graphical representation of the diffusion taking place. As discussed earlier, they begin at 0 (at time 0) and approach 1.0 (equilibrium) as time progresses.

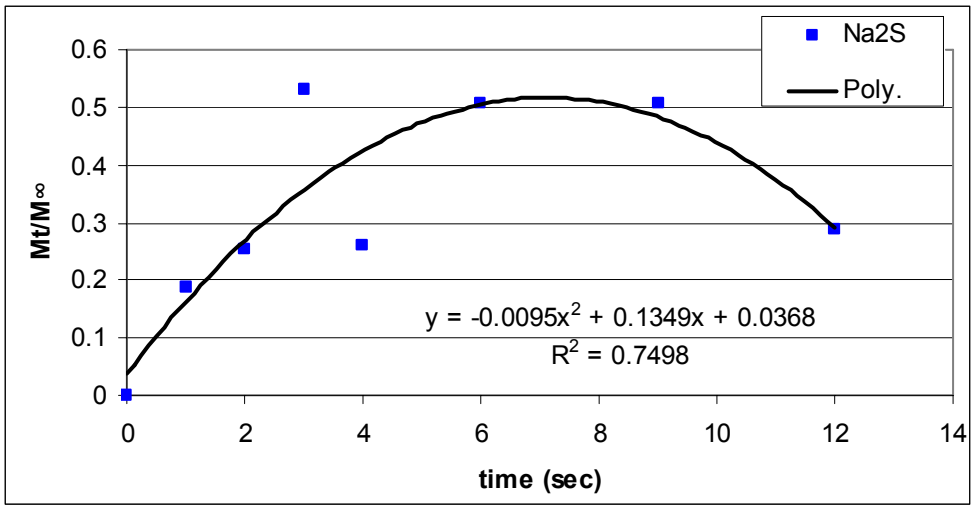

Figure 4.4.1: M_t / M_∞ Data for Run 9

Run 9 shows the M_t / M_∞ data for the diffusion measured with the 2.36 – 2.8mm fragments.

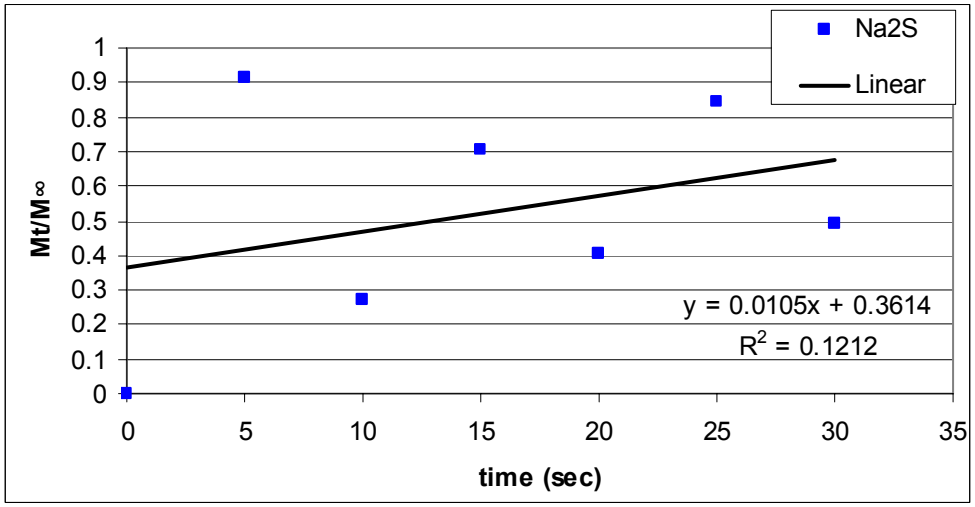

Figure 4.4.2: M_t / M_∞ Data for Run 10

Figure 4.4.2 above shows the M_t / M_∞ data for the larger 3.36 – 4.0mm fragments. A singular test was used, which may explain the variation in the data.

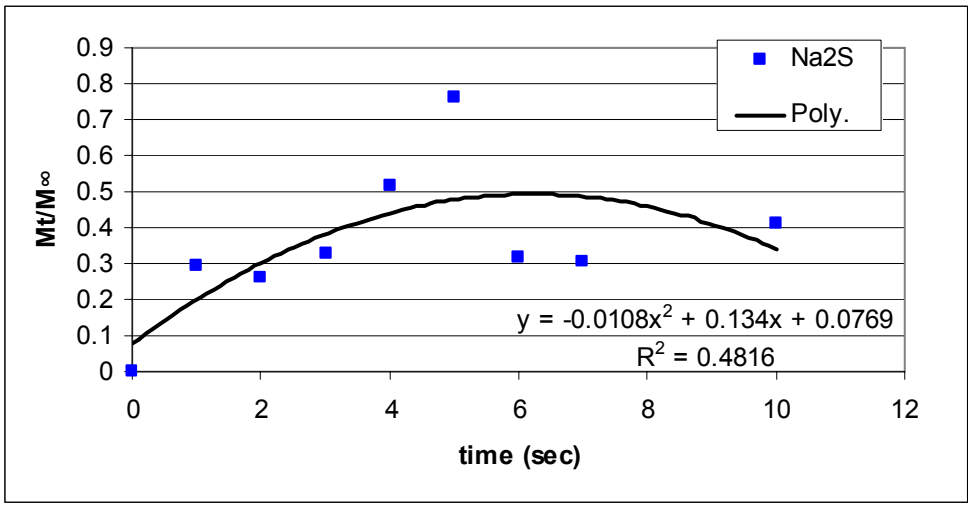

Figure 4.4.3: M_t / M_∞ Data for Run 11

Figure 4.4.3 above shows the M_t / M_∞ data for the larger 3.36 – 4.0mm fragments. In this experiment individual tests were run. The variation in the data is much lower.

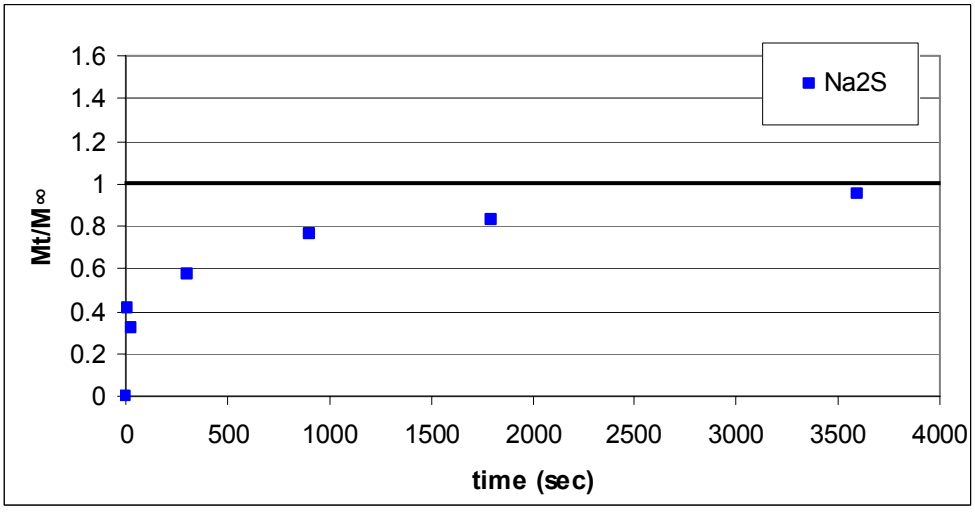

Figure 4.4.4: M_t / M_∞ Data for Run 13 – Short Time Zone

Figure 4.4.4 above shows the M_t / M_∞ data for the larger 3.36 – 4.0mm fragments in the long-term study. Here the short time zone is shown. In this experiment individual tests were run. The data shows a nice curve approaching the equilibrium of mixing.

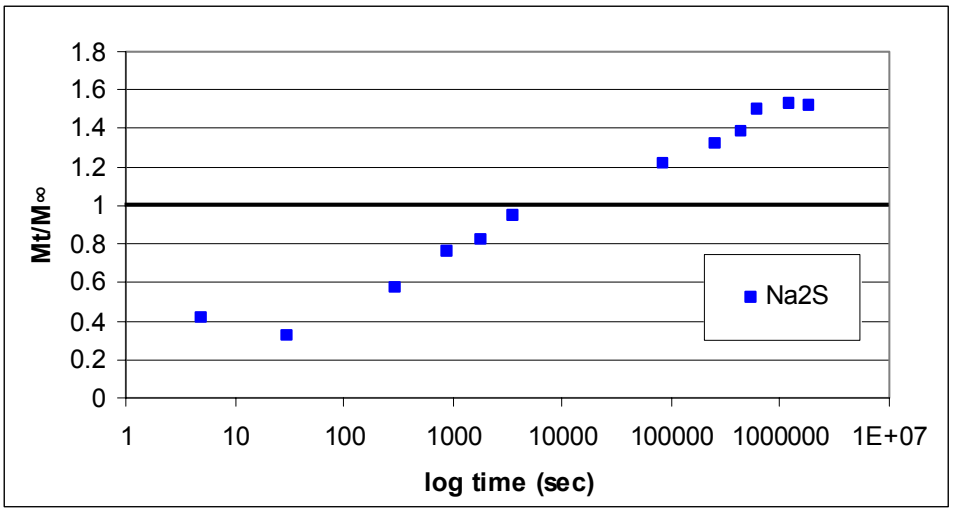

Figure 4.4.5: M_t / M_∞ Data for Run 13 – Long Time Zone

Figure 4.4.5 above shows the M_t / M_∞ data for the larger 3.36 – 4.0mm fragments in the long-term study. Here the entire data series is shown in a log scale. The M_t / M_∞ data increase quite linearly. However, after 3600 seconds it is clear that the data points increase past 1.0 peaking at 1.52. This is likely due to the binding of the sulfide to the lignin, increasing the diffusion past that of mixing alone. When the lignin binds to the fiber, the diffusion model used is no longer applicable. This data is shown to illustrate that equilibrium is reached fairly quickly, but over long periods of time binding occurs. Therefore, only the data points below 1.0 are used for analysis [46].

4.5 Image Analysis

Image analysis needed to be performed on the sampled fragments used in the experiments in order to calculate effective diffusivities that were accurate. Dimensional analysis would confirm that the sampled fragments were indeed cylindrical, confirming the cylindrical diffusion model proposed.

The length and width measurements were performed by ImageJ [45] via image analysis. The thickness measurement was performed manually by dial caliper. A spreadsheet was created to determine the equivalent radius of a cylindrical fragment that had the same diffusion characteristics of the actual rectangular fragments.

The smallest (0.5 – 1.0mm) fragments were not analyzed since they were not used for the effective diffusivity calculations.

4.5.1 Fragment Size 2.36 – 2.8mm

A random sample of 97 2.36 – 2.8mm fragments were collected as described in the procedure (section 3.2.3).

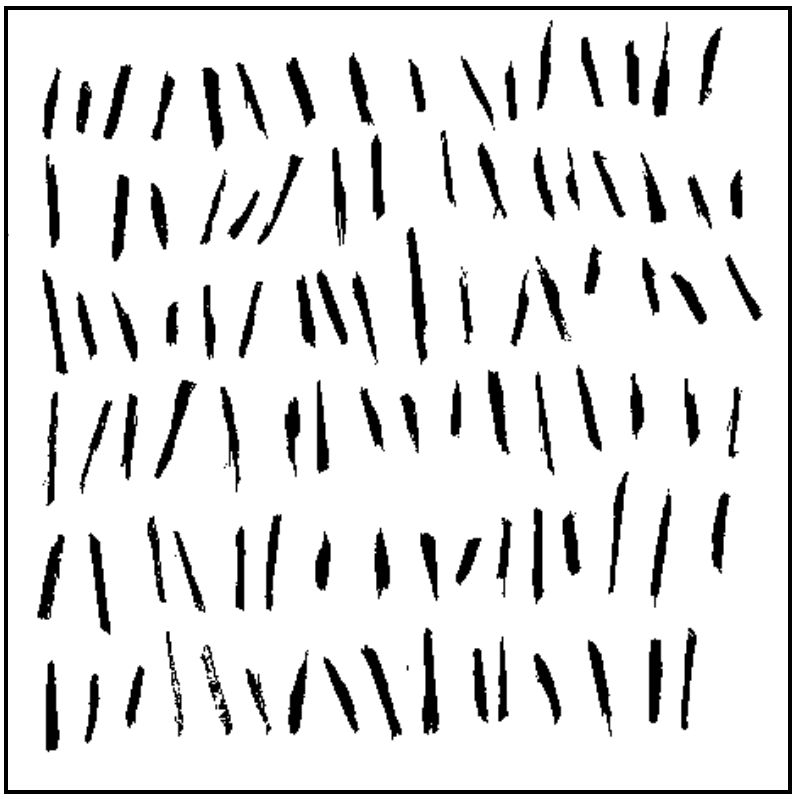

Figure 4.5.1.1: 8-bit Thresholded Image of 2.36 – 2.8mm Fragments

Figure 4.5.1.1 shows a graphical representation of the particle sizes encountered. The ruler has been removed for clarity, but a general idea of the size of the fragments can be determined. The "Edge" function was used in ImageJ to make the particles appear more clearly. The difference in size between the "Edge" data and the regular data is zero. The "Edge" function allows the particles to be viewed much more clearly. The average of the numbers obtained was used as this was virtually identical to the median.

The size data from ImageJ was inputted into the Excel spreadsheet for analysis. Solver was used to find the radius that minimized the sum of squares difference between the volumes of both objects at varying penetration depths. Table 4.5.1.1 summarizes this data.

Table 4.5.1.1: 2.36 – 2.8mm Fragment Sizes

Actual Dimensions		
Length	18.37	mm
Width	2.50	mm
Thickness	0.98	mm
Volume	45.01	mm^3
Surface Area	132.76	mm^2
Std Dev in Thickness	0.30	mm

Cylindrical Dimensions		
radius	0.63	mm
length	18.37	mm
Volume	23.15	mm^3
Surface area	75.63	mm^2
Standard Dev in r	0.17	mm

Table 4.5.1.1 shows that a radius of 0.63mm with the same length (18.37mm) will produce the same diffusion as the measured rectangular fragment. Although the volume and surface area are different between the two particles, the shape is the dominate factor in diffusion.

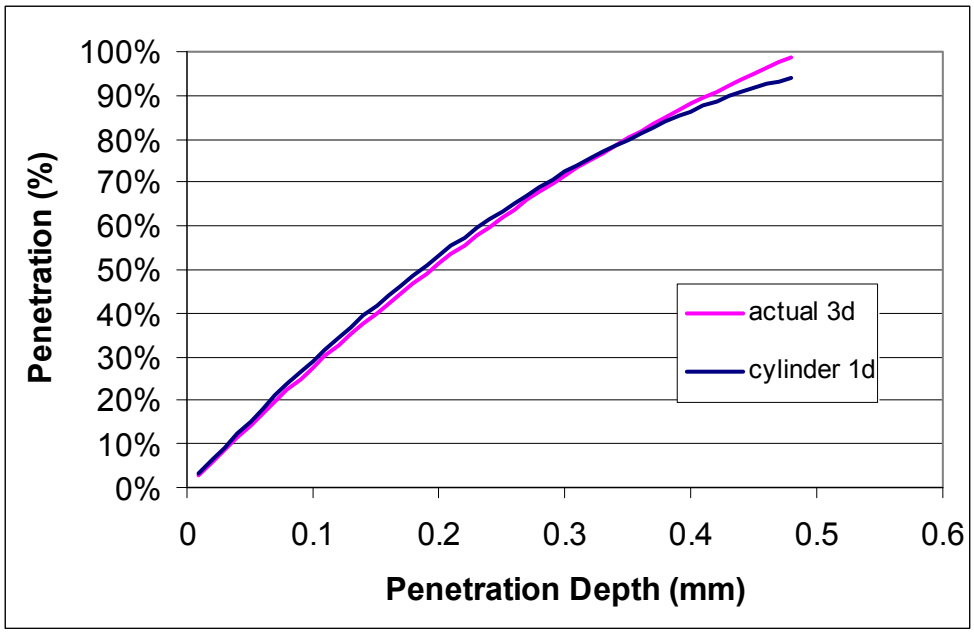

Figure 4.5.1.2: Model of Diffusion Through Actual 2.36 – 2.88mm Fragments versus Cylindrical

Figure 4.5.1.2 shows the difference between the cylindrical model and the diffusion through the actual 2.36 – 2.8mm fragment. Diffusion was calculated every 0.01mm through the entire fragment. Diffusion ends at 0.49mm of penetration as this is ½ the distance to the width of the rectangular fragment. At this point, the rectangular fragment is fully saturated. The figure shows that the difference between the two lines is very small. The difference in the range of 0.1-0.3mm penetration depth is only 1.9%. Although the model does diverge slightly in the end, the maximum difference here is only 3.9%.

This shows that the 2.36 – 2.8mm particles can indeed be modeled as cylinders and the maximum error in the resulting data will only be 3.9% different than if a rectangular diffusion model was used.

4.5.2 Fragment Size 3.36 – 4.0mm

A similar random sample of 96 3.36 – 4.0mm fragments were collected and analyzed per the procedure described.

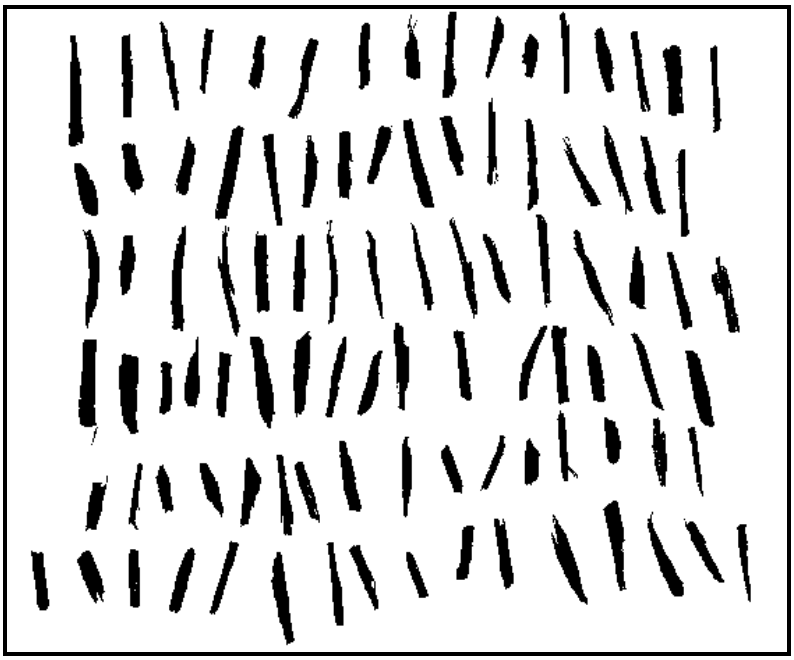

Figure 4.5.2.1: 8-bit Thresholded Image of 3.36 – 4.0mm Fragments

Figure 4.5.2.1 shows the thresholded image for the 3.36 – 4.0mm fragments. Although the ruler has been removed for clarity, the size of the particles in this image are much bigger. The "Edge" function in ImageJ was used to analyze these particles. The difference between the "Edge" and regular data is less than 1%.

The size data from ImageJ was inputted into the Excel spreadsheet for analysis similar to the method in section 4.5.1. Table 4.5.2.1 summarizes this data.

Table 4.5.2.1: 3.36 – 4.0mm Fragment Sizes

Actual Dimensions		
Length	21.75	mm
Width	3.39	mm
Thickness	1.15	mm
Volume	84.79	mm^3
Surface Area	205.29	mm^2
Std Dev in Thickness	0.27	mm

Cylindrical Dimensions		
radius	0.76	mm
length	21.75	mm
Volume	39.46	mm^3
Surface area	107.47	mm^2
Standard Dev in r	0.18	mm

Table 4.5.2.1 shows that a radius of 0.760mm with the same length (21.75mm) will produce the same diffusion as the measured rectangular fragment. As before, only the actual dimensions of the particle are relevant to diffusion.

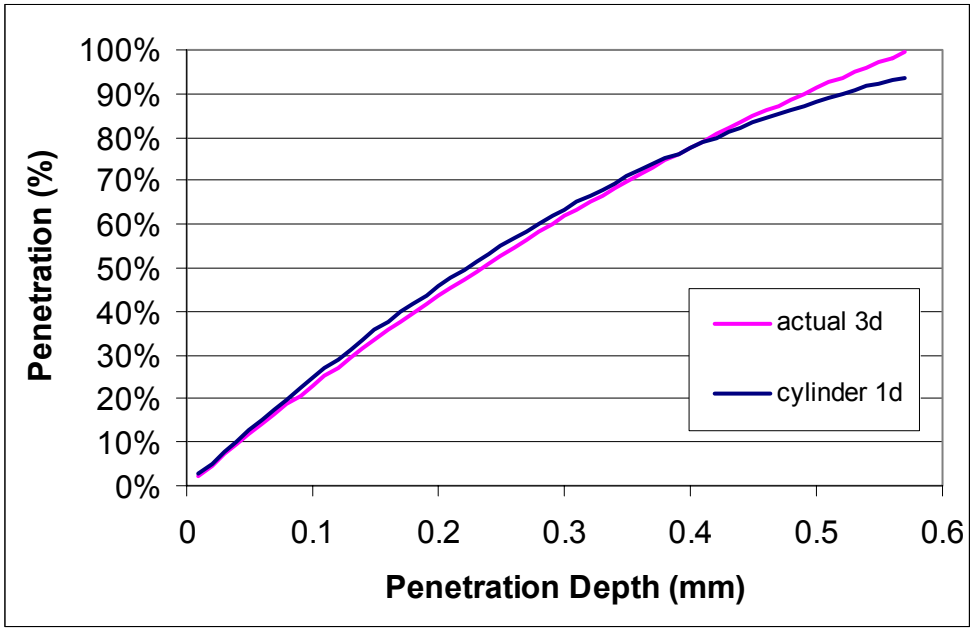

Figure 4.5.2.2: Model of Diffusion Through Actual 3.36 – 4.0mm Fragments versus Cylindrical

Figure 4.5.2.2 shows the difference between the cylindrical model and the diffusion through the actual 3.36 – 4.0mm fragment. Diffusion was calculated similar to section 4.5.1. Diffusion ends at 0.57mm of penetration as this is ½ the distance of the width of

the rectangular fragment. At this point, the rectangular fragment is fully saturated. The figure shows that the difference between the two lines is very small, but somewhat larger than the 2.36 – 2.88mm particles (Figure 4.5.1.2). The difference in the range of 0.1-0.4mm penetration depth is only 2.2%. Although the model does diverge slightly in the end, the difference here is only 4.8%.

This shows that the 3.36 – 4.0mm particles can indeed be modeled as cylinders and the maximum error in the resulting data will only be less than 5% different than if a rectangular diffusion model was used.

4.6 Effective Diffusivity Calculations

Effective diffusivities were calculated using the data from the M_t / M_∞ calculations. Runs 9, 10, 11, and 13 were analyzed and compiled into graphs based on the size fraction of the particles. The main curve represents the sum of squares best fit for the 1-dimensional diffusion model. The other two curves are the + / - 1 sigma standard deviation difference in the calculated radius based on the standard deviation of the measured thickness of the particle. This was done as a reference to the sensitivity of the data.

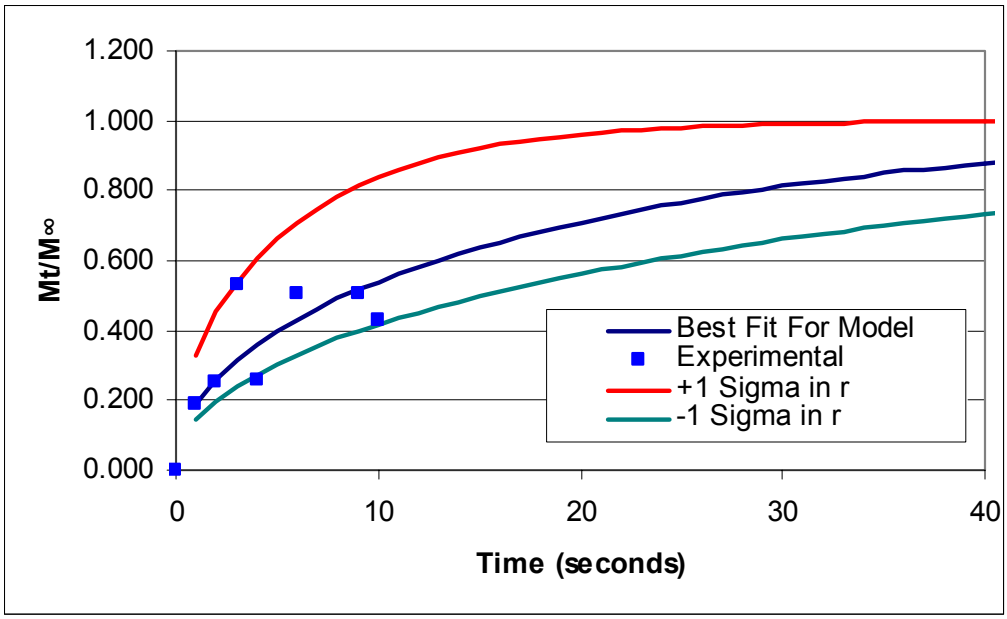

Figure 4.6.1: Effective Diffusivity Analysis for 2.36 – 2.8mm Fragments

Table 4.6.1: Calculated Effective Diffusion for 2.36 – 2.8mm Fragments

Size Fraction	Radius	D_e
(mm)	(mm)	x 10^{-05} cm^2 sec^{-1}
	0.92	7.52
2.36 – 2.8	**0.63**	**3.51**
	0.38	1.25

Figure 4.6.1 and Table 4.6.1 show the diffusion data for the 2.36 – 2.8mm fragments. The data fit within the + / - 1 sigma variation nicely. The cylindrical model reaches equilibrium at 165 seconds. The -1 sigma curve reaches equilibrium at 443 seconds and the +1 sigma curve reaches it in 30 seconds. From these curves, the effect of changing radius on the resulting diffusion profile can be observed. The resulting D_e calculated for the 2.36 – 2.88mm fragments was 3.51 x 10^{-5} cm^2 s^{-1} with variation from 1.25 – 7.52 x 10^{-5} cm^2 s^{-1}. These numbers are on the same order as the self-diffusion coefficient.

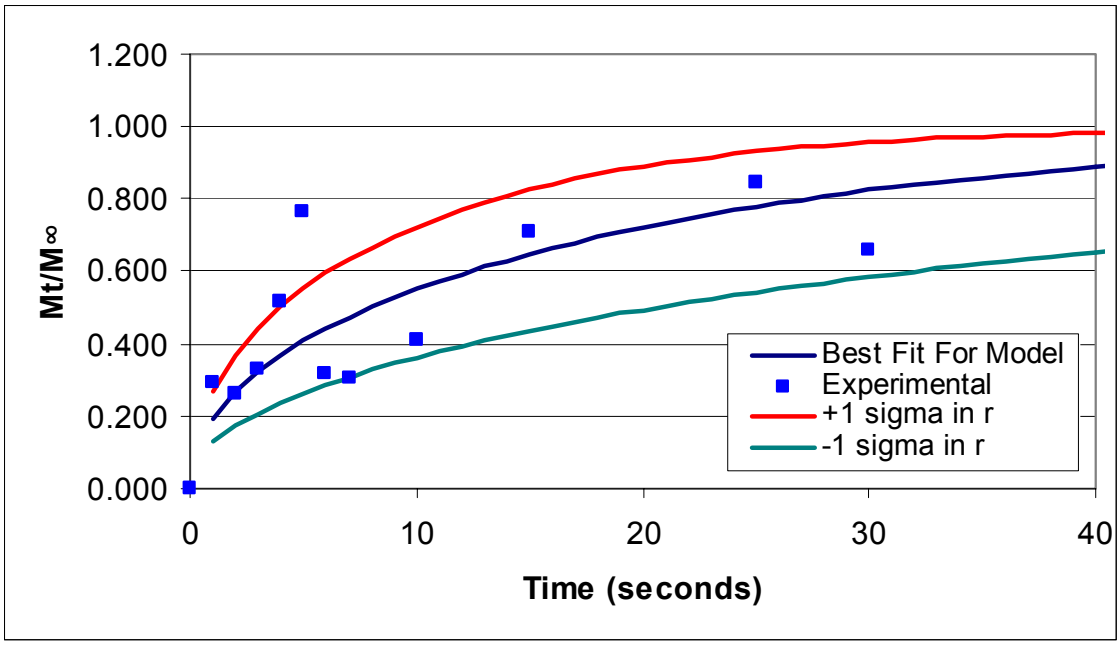

Figure 4.6.2: Effective Diffusivity Analysis for 3.36 – 4.0mm Fragments

Table 4.6.2: Calculated Effective Diffusion for 3.36 – 4.0mm Fragments

Size Fraction	Radius	D_e
(mm)	(mm)	x 10^{-05} cm^2 sec^{-1}
	1.06	9.20
3.36 – 4.0	**0.76**	**4.73**
	0.47	1.76

Figure 4.6.2 and Table 4.6.2 show the diffusion data for the 3.36 – 4.0mm fragments. The data fit within the + / - 1 sigma variation nicely. There are one or two data points that fall outside of the + / - 1 range, however they fall well within the + / - 2 sigma range. The cylindrical model reaches equilibrium at 159 seconds. The -1 sigma curve reaches equilibrium at 621 seconds and the +1 sigma curve reaches it in 40 seconds. Again, the effect of the changing radius is evident. The resulting D_e calculated for the 3.36 – 4.0mm fragments was 4.73 x 10^{-5} cm^2 s^{-1} with variation from 1.76 – 9.20 x 10^{-5} cm^2 s^{-1}. These numbers are on the same order as the self-diffusion coefficient.

4.7 Apparent Tortuosity Calculations

Tortuosity (τ) was calculated using the formula stated in section 3.2.5. Using the measured effective diffusivity (D_e) values, a porosity (ε) of 0.69, and the self-diffusion coefficient (D^o) of the HS^- ion (1.731×10^{-5} cm^2 s^{-1}) the tortuosity was calculated. Table 4.7.1 shows the results.

Table 4.7.1: Calculated Tortuosity Values

Size Fraction (mm)	Radius (mm)	D_e x 10^{-5} cm^2 s^{-1}	Apparent Tortuosity
	0.92	7.52	0.159
2.36 – 2.8	**0.63**	**3.51**	**0.340**
	0.38	1.25	0.956
	1.06	9.20	0.130
3.36 – 4.0	**0.76**	**4.73**	**0.253**
	0.47	1.76	0.679

Table 4.7.1 shows some key conclusions. One main point is that for the 2.36 – 2.8mm fragments the D_e calculated was 3.51×10^{-5} cm^2 s^{-1}. The larger 3.36 – 4.0mm fragments had a D_e of 4.73×10^{-5} cm^2 s^{-1}. This data is on the same order as the self-diffusion coefficient and on the same order as similar size particles. However, the tortuosity values are less than 1.0 since the measured D_e is greater than the self-diffusion coefficient of HS^-. This is the reason that apparent tortuosity is used. Figure 4.7.1 shows this graphically.

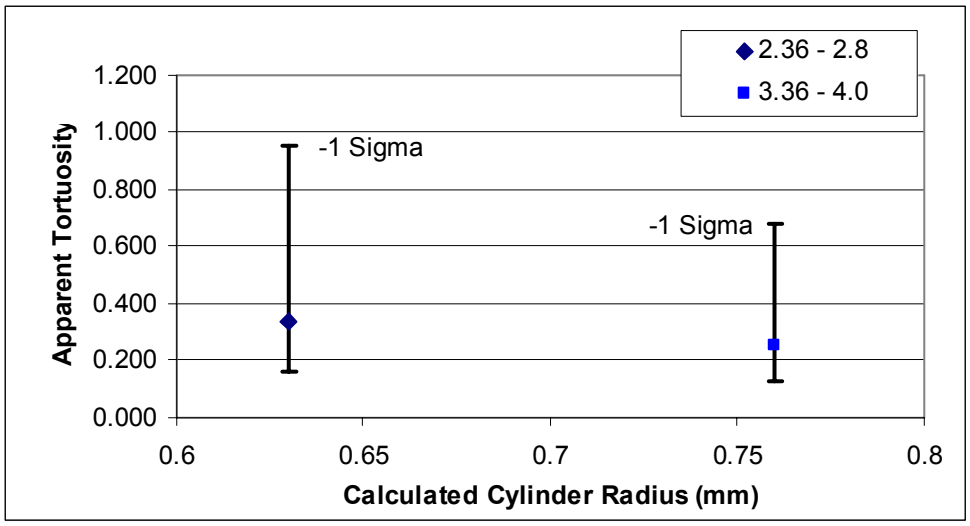

Figure 4.7.1: Apparent Tortuosity Values

This table also shows a trend of increasing tortuosity with decreasing particle size. Evidence supporting that tortuosity increases with decreasing particle size can be found in other work outside of the paper industry. Chitosan particles were studied for cadmium uptake and showed a similar relationship. Although the particles were modeled as spheres, they actually resemble flat discs. This change would increase the intake efficiency and would therefore be reflected in the change in tortuosity [48]. Also, the sulfation reaction on different limestone sorbents exhibited similar behavior for smaller particle sizes [49].

CHAPTER 5

DISCUSSION OF RESULTS

As mentioned before, the tortuosity value is only applicable to a particular system. However, it is useful in comparisons between systems.

Jacobson [29] studied the diffusion of tritiated water into 2.0 – 2.4mm pine fragments at 25 ºC. He found that the effective diffusion for this system was 1.11 x 10^{-5} cm^2 s^{-1} and the resulting tortuosity was 1.6. Here the tortuosity for this system is greater than one since the effective diffusion coefficient is lower than the self-diffusion coefficient. When compared to the data in this thesis, Na_2S diffuses much faster than water in the white liquor / wood system.

As an example of scale, the self diffusion coefficient of water at the same temperature (25 ºC) is 2.5 x 10^{-5} cm^2 s^{-1} [32]. The measured effective diffusion coefficients are larger than this. They are also much larger than the 1.731 x 10^{-5} cm^2 s^{-1} for the HS^- ion [32]. This is what causes the tortuosity to be less than 1.0. A tortuosity of less than 1.0 indicates that something other than Fickian diffusion is occurring. One explanation of this could be charge exclusion.

The example of tritiated water is a neutral system. That is, there are no charge effects since water is essentially neutral. Fibers are known to be anionic due to cellulose having a large amount of OH^- end groups [49, 50]. In this way, fibers act as a charged porous media [51]. However, the solution is not charged. The ionic strength of the OH^- groups with water is very small so no overall charge gradients are observed [50].

In the case of NaOH and cellulose, the ionic interactions are very large. In one study, the OH^- concentration in the inner solution of the cellulose was much lower than the

surrounding OH^- concentration. Increased OH^- concentrations magnified this result [50]. This effect occurs due to ion exclusion. Ion exclusion is the process of electrostatic repulsion of ions with like charge [51]. For example, the anionic charge on the surface of cellulose from a large amount of OH^- ions will repel the OH^- groups in the NaOH solution. In this way, the concentration inside the cellulose will be lower than the surrounding solution [50]. In this case, "anion exclusion" occurs due to the charge on the cellulose [51]. This is why NaOH does not adsorb readily with the fiber. It is also an explanation of why fibers swell in strongly alkaline solution [4]. Since the diffusing HS^- ions are repelled from the fiber as well, it is likely that they seek a path of lower resistance and diffuse by the anionic pores very quickly.

Since the tortuosity is a calculated number based on D_e and ε, the term "effective porosity" (ε_e) has been used to describe a system where charge effects occur. In uncharged media, the tortuosity is a geometric representation of the pore morphology. In charged systems, the pathways for cations and anions are different depending on the charge of the pore system [51]. This changes the porosity value of the individual ions, hence the term effective porosity. This also implies that there are a number of porosities depending on the number of components in the system. In a charged system such as this, the effective diffusivity of a charged ion would be considerably greater than in an uncharged system [51]. Again, since HS^- is charged it likely has a much higher effective porosity and therefore diffuses much quicker.

REFERENCES

1. Sjostrom, E., Wood Chemistry : Fundamentals and Applications, Academic Press, 2nd Edition (1993).

2. Smook, G. A., Handbook for Pulp and Paper Technologists, Angus Wilde Publications, 2nd Edition (1992).

3. Biermann, C. J., Handbook of Pulping and Papermaking, Academic Press, 2nd Edition (1996).

4. Kazi, K., Gauvin, H., Jollez, P., Chornet, E., "A Diffusion Model for the Impregnation of Lignocellulosic Materials," TAPPI Journal, v. 80, n. 11, p. 209 – 219 (1997).

5. Nevell, T., Zeronian, S., Cellulose Chemistry and Its Applications, Ellis Horwood (1985).

6. Stamm, A., "Passage of Liquids, Vapors, and Dissolved Materials through Softwoods", Tech. Bulletin 929, USDA, Washington, D.C. (1946).

7. Chavonda, J., Venditti, R., Joyce, T., "Effect of Enzymatic Pretreatment on the Diffusion of Sodium Hydroxide in Wood," TAPPI Journal, v.81, n. 1, p. 260 – 266 (1998).

8. Kollmann, F., Cote, W., Principles of Wood Science and Technology Vol. 1 : Solid Wood, Springer – Verlag (1968).

9. George, T., Science and Technology of Wood, Van Nostrand Reinhold (1991).

10. Tiemann, D. H., Wood Technology, Pitmann (1947).

11. Ingruber, O. V., Kocurek, M. J., Wong, A., Pulp and Paper Manufacture Vol. 4 : Sulfite Science and Technology, TAPPI Press, 3rd Edition (1985).

12. Beazley, W. B., Johnston, H. W., Maass, O., "The Penetration into Wood of Cooking Liquors and Other Media," Dominion Forest Service Bulletin 95, Canada Dept. of Mines and Resources (1939).

13. Rydholm, S., Pulping Processes, Wiley and Sons (1965).

14. Stenius, Per, Forest Products Chemistry, TAPPI Press (2000).

15. Ban, W., Lucian, L., "Enhancing Kraft Pulping through Unconventional Higher Sulfide-Containing Pretreatment Liquors – A Review," TAPPI Journal, v. 2, n. 3, p. 1 – 26 (2003).

16. Licht, S., Manassen, J., "The Second Dissociation Constant of H_2S," J. Electro Chem. Soc., v. 134, p. 918 (1987).

17. Vanchinathan, S., Krishnagopalan, G., "Kraft Delignification Kinetics Based on Liquor Analysis," TAPPI Journal, v. 78, n. 3, p. 127 – 132 (1995).

18. Gierer, J., J. Wood Sci. Technol., v.14, n.4, p. 241 (1980).

19. Li, Z., Kubes, G., "Kinetics of Delignification and Cellulose Degradation During Pulping with Polysulfide and Anthraquinone," J. Pulp and Paper Sci., v. 28, n. 7, p.234 – 239 (2002).

20. Wilder, H., Daleski, E., TAPPI Journal, v. 48, n. 5, p.293 (1965).

21. Vanchinathan, S., Krishnagopalan, G., "Dynamic Modeling of Kraft Pulping of Southern Pine Based on On-Line Liquor Analysis," TAPPI Journal, v. 80, n. 3, p. 123 – 133 (1997).

22. Biasca, Kayrn, "A Survey of Pulp Mill Use of Anthraquinone," TAPPI Journal, v.81, n. 1, p. 78 – 79 (1998).

23. MacLeod, M., Radiotis, T., Uloth, V., Munro, F., Tench, L., "Basket Cases IV : Higher Yield with Paprilox Polysulfide – AQ Pulping of Hardwoods," TAPPI Journal, v. 1, n. 8, p.3 – 8 (2002).

24. Hines, A., Maddox, R., Mass Transfer : Fundamentals and Applications, Prentice – Hall (1985).

25. Jaaskelainen, A., Poppius-Levlin, K., "Mass Transfer in Peroxyacetic Acid Bleaching of Kraft Pulp," TAPPI Journal, v. 84, n. 8, p.1 – 10 (2001).

26. Deen, W., Analysis of Transport Phenomena, Oxford University Press (1998).

27. "Essentials of Bessel Functions," http://www.du.edu/~jcalvert/math/bessels.htm

28. Crank, J., The Mathematics of Diffusion, Claredon Press (1975).

29. Jacobson, A. J., Banerjee, S., "Diffusion of Tritiated Water into Water-Saturated Wood Particles," Submitted for Publication.

30. Van Der Kamp, G., Stempvoort, D. R., Wassenaar, L. I., "The Radial Diffusion Method: Using Intact Cores to Determine Isotopic Composition, Chemistry, and

Effective Porosities for Groundwater in Aquitards," Water Resources Research, v. 32, p.1815 – 1822 (1996).

31. Isenberg, I.H., Pulpwoods of the United States and Canada – Conifers, Vol. 1, The Institute of Paper Chemistry (1980).

32. Perry, R. H., Green, D. W., Perry's Chemical Engineers' Handbook, McGraw – Hill, 7th Edition (1997).

33. Ban, W., Singh, J., Wang, S., Lucia, L., "Kraft Green Liquor Pretreatment of Softwood Chips Part II : Chemical Effect on Pulp Carbohydrates," J. Pulp and Paper Sci., v. 29, n. 4, p.114 – 119 (2003).

34. Svedman, M., Tikka, P., "The Use of Green Liquor and its Derivatives in Improving Kraft Pulping," TAPPI Journal, v. 81, n. 10, p.151 – 158 (1998).

35. Jameel, H., Gratzl, J., Prasad, D., Chivukula, S., "Extending Delignification with AQ/Polysulfide," TAPPI Journal, v. 78, n. 9, p.151 – 160 (1995).

36. Mao, B., Hartler, N., "Improved Modified Kraft Cooking," TAPPI Journal, v. 77, n. 11, p.149 – 153 (1994).

37. Jiang, J., "Extended Modified Cooking of Southern Pine with Polysulfide : Effects on Pulp Yield and Physical Properties," TAPPI Journal, v. 77, n. 2, p.120 – 124 (1994).

38. Thompson, R., Paleologoli, M, Jemma, N., Wong, Y., Uloth, V., "Electrodialysis Separates a Sulfide – Rich Liquor from Mill White Liquor," TAPPI Journal, v. 81, n. 10, p.159 – 164 (1998).

39. Tench, L., Uloth, V., Dorris, G., Hornsey, D., Munro, F., "Mill – Scale Implementation of Paprican's Process for Polysulfide Liquor Production in Kraft Mill Causticizers," TAPPI Journal, v. 82, n. 10, p. 120 – 129 (1999).

40. Uloth, V., Dorris, G., Thring, R., Hogikyan, "Production of Polysulfide Liquor in a Kraft Mill's Causticizers," TAPPI Journal, v. 80, n. 10, p.223 – 233 (1997).

41. Watanabe, K., Andoh, T., Shimizu, M., Shimohira, T., "New Process Produces Highly Concentrated Polysulfide Liquor by Electrolysis of White Liquor," TAPPI Journal, v. 84, n. 2, p.1 – 14 (2001).

42. Sturgeoff, L., Pitl, Y., "Low-Kappa Pulping Without Capital Investment : Using Anthraquinone for Low-Kappa Pulping," TAPPI Journal, v. 77, n. 7, p.95 – 100 (1994).

43. "Moisture in Pulp, Paper, and Paperboard," TAPPI Test Method T 412 om – 02 (2002).

44. "Analysis of Soda and Sulfate White and Green Liquors," TAPPI Test Method T 624 cm – 00 (2000).

45. Rasband, W. S., ImageJ, National Institutes of Health, Bethesda, Maryland, USA, http://rsb.info.nih.gov/ij, 1997 – 2004.

46. Ban, W., Song, J., Lucia, L., "Insight into the Chemical Behavior of Softwood Carbohydrates during High-Sulfidity Green Liquor Pretreatment," Ind. Eng. Chem. Res., v. 43, p.1366 – 1372 (2004).

47. Evans, J. R., Davids, W. G., MacRae, J. D., Amirbahman, A., "Kinetics of Cadmium Uptake by Chitosan – Based Crab Shells," Water Res., v. 36, p.3219 – 3226 (2002).

48. Adanez, J., Gayan, P., Garcia – Labiano, F., "Comparison of Mechanistic Models for the Sulfation Reaction in a Broad Range of Particle Sizes of Sorbents," Ind. Eng. Chem. Res., v. 35, p.2190 – 2197 (1996).

49. Larsson, P., "Dissolution of Lignin in Kraft Pulp by Oxygen Bleaching," J. Wood Sci. Chem. and Tech., v. 13, n. 2, p.237 – 259 (1993).

50. Motomura, H., Bae, S., Morita, Z., "Dissociation of Hydroxyl Groups of Cellulose at Low Ionic Strengths," Dyes and Pigments, v. 39, n.4, p.243 – 258 (1998).

51. Smith, D., Pivonka, P., Jungnickel, C., Fityus, S., "Theoretical Analysis of Anion Exclusion and Diffusive Transport Through Platy – Clay Soils," Transport in Porous Media, v. 57, p.251 – 277 (2004).